

THREE-DIMENSIONAL SUPERVIRTUAL SEISMIC REFRACTION
INTERFEROMETRY

BY
EDIGBUE, PAUL IRIKEFE

A Thesis Presented to the
DEANSHIP OF GRADUATE STUDIES

KING FAHD UNIVERSITY OF PETROLEUM & MINERALS

DHAHRAN, SAUDI ARABIA

In Partial Fulfillment of the
Requirements for the Degree of

MASTER OF SCIENCE

In
GEOPHYSICS

NOVEMBER 2015

KING FAHD UNIVERSITY OF PETROLEUM & MINERALS
DHAHRAN 31261, SAUDI ARABIA

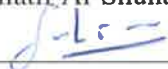
DEANSHIP OF GRADUATE STUDIES

This thesis, written by **EDIGBUE, PAUL IRIKEFE** under the direction of his thesis advisor and approved by his thesis committee, has been presented to and accepted by the Dean of Graduate Studies, in partial fulfillment of the requirements for the degree of **MASTER OF SCIENCE IN GEOPHYSICS**.

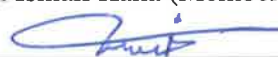
Thesis Committee



Dr. Abdullatif Al-Shuhail (Advisor)



Dr. SanLinn Ismail Kaka (Member)



Dr. Khalid Al-Ramadan (Member)



Dr. Abdulaziz Al-Shaibani

Department Chairman



Dr. Salam A. Zummo

Dean of Graduate Studies

3/12/15

Date



©Edigbue, Paul Irikefe
2015

Dedication

To my late father for his prayers and support.

ACKNOWLEDGMENTS

I acknowledge the contributions of all those who shared in the success of this thesis.

Their contributions really made the success of this work possible.

Dr. Abdullatif Al-Shuhail: I wish to express my sincere gratitude to Dr. Al-Shuhail, my supervisor and academic mentor, for his lovely and fatherly guidance, stimulating suggestions, advice and evaluation in putting together this thesis and for his tremendous support throughout the course of this study. You are very precious to me, thank you so much sir.

Dr. SanLinn Ismail Kaka: I thank Dr. Kaka for his expertise support and for his unforgettable kindness during the period of this thesis preparation.

Dr. Khalid Al-Ramadan: I thank Dr. Al-Ramadan for his contribution, encouragement and useful suggestions.

Dr. Abdullaziz Shaibani: I convey special thanks to Dr. Shaibani, the Chairman, Earth Sciences Department, for his leadership, immense support and contribution towards the success of my program in KFUPM.

Professor Gabor Korvin: I thank Prof. Korvin for his unforgettable kindness throughout my stay in KFUPM, and for his fatherly care, support and advice

at all times.

Nigerian Community and friends: I thank my many friends from the Nigerian community for their leadership, support, care, advice and companionship.

Saudi Arabian Government: I acknowledge the generosity of the Saudi Arabian Government, through the Ministry of Higher Education, for providing a scholarship to complete my master's program.

TABLE OF CONTENTS

| | Page |
|----------------------------------------------------------|-------------|
| ACKNOWLEDGEMENTS | iii |
| LIST OF TABLES | vii |
| LIST OF FIGURES | viii |
| ABSTRACT (ENGLISH) | x |
| ABSTRACT (ARABIC) | xii |
| CHAPTER 1 INTRODUCTION | 1 |
| 1.1 Introduction | 1 |
| 1.2 Statement of Problem | 3 |
| 1.3 Objectives | 6 |
| 1.4 Justification of the Study | 6 |
| 1.5 Benefits of the Study | 6 |
| 1.6 Structure of the Thesis | 7 |
| CHAPTER 2 LITERATURE REVIEW | 9 |
| 2.1 General Overview | 9 |
| 2.2 Previous Studies of Seismic Interferometry | 10 |
| 2.3 Previous Studies of Supervirtual Method | 12 |
| CHAPTER 3 METHODOLOGY | 15 |

| | | |
|--------------------------------------------------|------------------------------------------------------------------------|-----------|
| 3.1 | Theory | 15 |
| 3.2 | Synthetic 3D Seismic Refraction | 22 |
| 3.2.1 | Synthetic 3D Seismic Refraction Description | 22 |
| 3.2.2 | Synthetic 3D seismic refraction data generation | 25 |
| 3.3 | The 3D Supervirtual Seismic Refraction Interferometry Method | 29 |
| 3.3.1 | Crosscorrelation | 29 |
| 3.3.2 | Alignment | 30 |
| 3.3.3 | Summation | 30 |
| 3.3.4 | Semi-Automatic First-Arrival Calculation Method | 31 |
| CHAPTER 4 RESULT AND DISCUSSION | | 33 |
| 4.1 | Overview | 33 |
| 4.2 | Results of Noiseless 3D Synthetic Seismic Refraction Data | 34 |
| 4.3 | Supervirtual Methods | 43 |
| 4.4 | Analysis of Results | 50 |
| CHAPTER 5 CONCLUSIONS AND RECOMMENDATIONS | | 54 |
| 5.1 | Conclusions | 54 |
| 5.2 | Recommendations | 55 |
| REFERENCES | | 57 |
| VITAE | | 61 |

LIST OF TABLES

| | | |
|-----|---------------------------------------------------------------------------------------------|----|
| 4.1 | True first arrivals at all receivers of line 1 from sources 1, 43 and 105 . . | 38 |
| 4.2 | Extracted first arrivals from raw synthetic data and after supervirtual method | 51 |

LIST OF FIGURES

| | | |
|-----|-------------------------------------------------------------------------------------------------------------------------------------|----|
| 1.1 | Raw data example, showing high level of noise on the farthest offsets (adapted from Seimetz et al. (2013)) | 5 |
| 3.1 | Schematic diagram showing reflected ray, direct ray and the critically refracted rays which also known as the head wave. | 17 |
| 3.2 | Schematic Diagram of Supervirtual Traces: (a) Crosscorrelation; (b) Convolution; (c) Summation. | 18 |
| 3.3 | 3D layout used to generate synthetic data | 24 |
| 3.4 | Zero phase wavelet | 26 |
| 3.5 | 3D sources and receivers layout for 2 layer case | 28 |
| 3.6 | Flowchart of 3D Semi-Automatic Method | 32 |
| 4.1 | Noiseless traces at source 1: (a) receiver line 1; (b) receiver line 3; (c) receiver line 5. | 35 |
| 4.2 | Noiseless traces at source 43: (a) receiver line 1; (b) receiver line 3; (c) receiver line 5. | 36 |
| 4.3 | Noiseless traces at source 105: (a) receiver line 1; (b) receiver line 3; (c) receiver line 5. | 37 |
| 4.4 | Noisy traces at source 1: (a) receiver line 1; (b) receiver line 3; (c) receiver line 5. | 40 |
| 4.5 | Noisy traces at source 43: (a) receiver line 1; (b) receiver line 3; (c) receiver line 5. | 41 |
| 4.6 | Noisy traces at source 105: (a) receiver line 1; (b) receiver line 3; (c) receiver line 5. | 42 |

| | | |
|------|--------------------------------------------------------------------------------------------------------------------------------------|----|
| 4.7 | Crosscorrelated traces of receiver line 1 from: (a) source 1; (b) source 43; (c) source 105. | 44 |
| 4.8 | Aligned crosscorrelated traces of receiver line 1 from: (a) source 1; (b) source 43; (c) source 105. | 45 |
| 4.9 | Stacked trace of receiver line 1 from: (a) source 1; (b) source 43; (c) source 105. | 47 |
| 4.10 | Enhanced traces of receiver line 1 from: (a) source 1; (b) source 43; (c) source 105. | 48 |
| 4.11 | Amplitude comparison between noisy and enhanced traces of receiver line 1 from: (a) source 1; (b) source 43; (c) source 105. | 49 |
| 4.12 | First arrival comparison between noiseless traces of receiver line 1 from: (a) source 1; (b) source 43; (c) source 105. | 52 |
| 4.13 | Plots of % error against trace numbers of receiver line 1 from: (a) source 1; (b) source 43; (c) source 105. | 53 |

THESIS ABSTRACT

NAME: Edigbue, Paul Irikefe

TITLE OF STUDY: THREE-DIMENSIONAL SUPERVIRTUAL SEISMIC REFRACTION INTERFEROMETRY

MAJOR FIELD: Geophysics

DATE OF DEGREE: November 2015

The quality of seismic data is often distorted by many types of near-surface features, nearby cultural noise and far offset problem. This is a prominent phenomenon, with data from areas of complex geology such as a cavity, undulating subsurface topography, faults and fractures. These geologic features cause lateral and vertical variations in subsurface layer velocity which result into variations in travel time of the seismic refraction signal. Supervirtual interferometry (SVI) methods enhance the signal-to-noise ratio (SNR) of noisy seismic refraction data. However, the conventional 2D SVI methods have the limitation of ray-path problem when applied directly on 3D case. In this study, I extend the supervirtual seismic refraction interferometry method to 3D geometries commonly used in active seismic exploration. To achieve this objective, synthetic 3D seismic refraction data were created using single patch orthogonal geometry with

5 receiver lines and 5 source lines. Each source line has 21 sources and each receiver line has 21 receivers. Simple two-velocity model ($V_1 = 500\text{m/s}$, $V_2 = 2500\text{m/s}$) was used. A zero phase wavelet was convolved with the refraction travel time to create the seismic wiggle trace. Gaussian random noise with zero mean and 0.25 standard deviation was added to simulate a case of moderate ambient noise. The data was separated into receiver lines for each shot record. The supervirtual algorithm, consisting of crosscorrelation, alignment, summation and first arrival calculation is performed. By aligning and summation of all the correlogram, the stationary position of source-receiver pairs as required in the 2D supervirtual method are eliminated in this case. This 3D supervirtual algorithm enhances SNR and is helpful in removal of side lobes cause by convolution. Synthetic data presented in this study shows accurate first arrivals after the application of the 3D SVI and traces with much better SNR than the actual traces.

Abstract-Arabic

تتأثر جودة البيانات السيزمية سلباً بأنواع مختلفة من الأعراض القريبة من السطح كالضجيج الصادر من البشر و المشاكل التي تحدث بسبب بعد المسافة للمستقبلات السيزمية بالمقارنة بالعمق المراد استكشافه. هذا التأثير هو ظاهرة بارزة مع البيانات المأخوذة من أماكن ذات خصائص جيولوجية معقدة كالتجاويف و التضاريس المتموجة تحت السطح و الصدعات و الشقوق. هذه الخصائص الجيولوجية تسبب تغييرات في السرعة تحت سطحية للموجات أفقياً و عمودياً مما يؤدي إلى اختلافات في الوقت المطلوب لانتقال إشارة الانكسار السيزمي. الأساليب المسماة Supervirtual interferometry أو ما يطلق عليه اختصاراً SVI تحسن نسبة الإشارة إلى الضوضاء في بيانات الانكسار السيزمي ذات الضوضاء العالي. و مع ذلك فإن أساليب SVI التقليدية ثنائية الأبعاد لديها قصور في مشكلة طريق الإشعاع عند تطبيقها مباشرة على حالة ثلاثية الأبعاد. في هذه الدراسة قمت بتمديد استخدام أسلوب SVI للانكسار السيزمي إلى الحالات ثلاثية الأبعاد التي يشيع استخدامها في مجال الاستكشاف السيزمي. لتحقيق هذا الهدف، تم إنشاء بيانات الانكسار السيزمي ثلاثية الأبعاد الصناعية باستخدام مساحة بحث متعامدة دفعة واحدة بخمس خطوط مستقبلات و خمس خطوط مصادر إرسال. كل خط من خطوط المستقبلات فيه 21 مستقبل و كل خط من خطوط المصادر فيه 21 مصدر إرسال. تم استخدام نموذج بسيط بسرعتين، السرعة الأولى 500 متر في الثانية و السرعة الثانية 2500 متر في الثانية. تم عمل الالتفاف (convolution) للموجات ذات الطور الموجي الصفري مع الوقت المطلوب لانتقال إشارة الانكسار السيزمي لخلق أثر التذبذب السيزمي. كما تمت إضافة ضجيج جافس عشوائي له معدل صفر و انحراف معياري 0.25 لمحاكاة حالة ذات ضوضاء محيطية معتدلة. تم فصل البيانات إلى خطوط المستقبلات لكل سجل. تم تنفيذ خوارزمية SVI المتكونة من محاذاة و جمع و حساب أول وصول. عن طريق المحاذاة و الجمع يتم التخلص من متطلب أسلوب SVI ثنائي الأبعاد الذي يقتضي بثبات المستقبلات و مصادر الإرسال. هذه الخوارزمية لأسلوب SVI ثلاثي الأبعاد تحسن نسبة الإشارة إلى الضوضاء و تفيد في إزالة الفصوص الجانبية التي يتسبب بها الالتفاف. البيانات الاصطناعية الواردة في هذه الرسالة تبين دقة الوصول الأولي بعد تطبيق أسلوب SVI ثلاثي الأبعاد، كما تبين تحسن نسبة الإشارة إلى الضوضاء عن السابق.

CHAPTER 1

INTRODUCTION

1.1 Introduction

The quality of near-surface seismic data is expected to improve with modern acquisition design and array of geophones. In spite of the progress made in seismic surveying, seismic data still suffer from poor quality, especially data collected in areas with complex near-surface geology. Such conditions result in data showing improper imaging of geologic structures. This distortion of near-surface seismic signals occurs as a result of complex subsurface topography, varying lateral velocity and noise traveling within the near surface layer. Areas where this geologic problem occurs pose great challenges to exploration activities. This poor data quality problem damps the effectiveness of traditional processing methods. Therefore, it became imperative to enhance the signal-to-noise ratio (SNR) of data with this peculiar problem before processing and interpretation.

Near-surface records resulting from complex overburden can be imaged using the vir-

tual source method (Bakulin and Calvert, 2004). Korneev et al. (2008) used virtual source method to image complex overburden and they applied the technique to synthetic data acquired from model typical of Middle East structures.

There are many methods for improving data quality from near-surface records including seismic interferometry. For instance, Akram and Eaton (2014) proposed an algorithm based on repetitive crosscorrelation to improve arrival time picking. Seismic interferometry has been used for enhancing the signal-to-noise ratio of seismic data (Al-Shuhail et al., 2013). The concept is to merge waveform, recorded at different receivers to generate the wave that would travel between these receivers if one of these receivers was a source. This eliminates the need to have a source located at each receiver positions. Seismic interferometry utilizes the crosscorrelation of a trace pair to reproduce the Green's function between them. The resulting Green's functions are stacked to produce an enhanced version of Green's function between the receiver pair. Previous studies (e.g., Nicolson (2011); Nicolson et al. (2012); Kang (2014); Liu et al. (2014); Al-Shuhail (2015)) have used the technique of seismic interferometry to image complex subsurface structures successfully.

This thesis focuses on the use of seismic interferometry algorithm proposed adapted from Al-Shuhail et al. (2013) and Al-Shuhail (2015) to enhance first arrivals on active 3D seismic data. Applying the conventional 2D SVI on 3D seismic refraction data suffers a setback because the 2D SVI assumed a stationary position for source-receiver pairs which is not applicable in 3D case. Lu et al. (2014) proposed 3D SVI algorithm which generates virtual and supervirtual traces and integrate them along source and

receiver lines respectively before stacking. I have proposed 3D SVI method that improve the generation of supervirtual traces. This algorithm considers the alignment of correlograms, generated from crosscorrelating all traces, to common time. Based on this concept, all traces from the 3D seismic refraction data could be considered at the same time regardless of their receiver or source lines. Therefore, this study proposes a modified 3D supervirtual interferometry algorithm which includes; crosscorrelation, alignment, summation and first-arrival calculation.

1.2 Statement of Problem

Most near-surface seismic data has low SNR at far offset (Figure 1.1), and are distorted by certain geologic features in the subsurface, which poses challenges in first arrival picking during data processing and interpretation. These geologic features cause lateral and vertical variations in subsurface layer velocity which result into variations in travel time of the seismic refraction signal, and noisy data. There is a need to enhance the first arrival of noisy seismic data. This will enable the first arrival picking to be carried out automatically at better confidence level without necessarily discarding most challenging seismic data. Several studies (Alshuhail et al., 2012; Al-Shuhail et al., 2013; Al-Shuhail, 2015) tackled this problem, however, these studies cannot be applied directly to active 3D seismic data. Al-Shuhail et al. (2013) and Al-Shuhail (2015) developed algorithms which were used successfully to enhance the first arrival of microseismic data and improve automatic picking of first arrivals of 2D seismic data, respectively. The 2D SVI methods has the limitation of ray-path problem when applied directly on

3D case (Lu et al., 2014). I have proposed 3D SVI algorithm which adequately takes care of ray-path problem. Therefore, this study focuses on the extension of the above algorithms to operate on 3D seismic geometries commonly used in petroleum seismic exploration surveys.

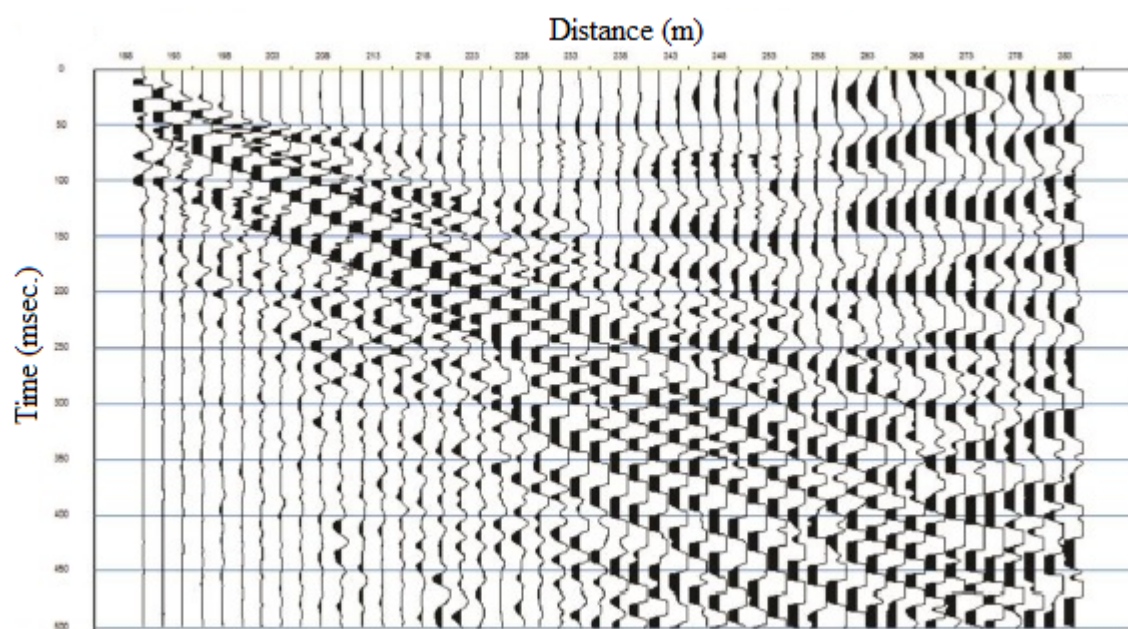


Figure 1.1: Raw data example, showing high level of noise on the farthest offsets (adapted from Seimetz et al. (2013))

1.3 Objectives

The objective of this study are as follows:

- Extending the supervirtual refraction interferometry method to operate on 3D active seismic data.
- Generating low profile synthetic 3D seismic data to test the enhance first arrival picking algorithm, using orthogonal survey method.
- Estimating the SNR of the enhanced data and postulate the basis for comparison of the noisy and enhanced first arrivals.

1.4 Justification of the Study

Previous studies, such as Al-Shuhail et al. (2013) and Al-Shuhail (2015), show that first arrival picking could be improved using interferometry techniques. Their methods were tested on microseismic, synthetic 2D and real 2D seismic data. This study is motivated by the need to extend the first arrival enhancement algorithm from previous studies to operate on 3D active seismic data which is commonly used in the petroleum industry.

1.5 Benefits of the Study

The success of seismic imaging of geologic features depends largely on the data quality. Data quality enhancement contributes to the tremendous success achieved in subsurface imaging. For seismic refraction surveys where the primary issue is first arrival picking,

its data quality still needs to be improved for accurate arrival time picking. In seismic data processing, enhancement of the first arrival reduces the risk associated with processing noisy data and optimizes the first arrival picking time. Processes such as filtering and amplitude gain become unnecessary when the first arrival is adequately enhanced. Also, first arrival enhancement will preserve the shape of seismic wave and amplitude which are very important in imaging subsurface structures.

During interpretation of seismic refraction data, first arrival picking is an important factor, to preserve its accuracy, its picking is carried out automatically with the data enhancement algorithm. Subsurface topography is better delineated with enhanced data quality, which is easily achieved with the enhancement of the first arrival. The 3D supervirtual seismic refraction algorithm will promote first arrival enhancement of 3D seismic refraction and hence its quality of interpretation will improve. More 3D seismic refraction data acquisition will be carried out since the algorithm to handle it is available.

1.6 Structure of the Thesis

The thesis is organized into five chapters.

Chapter 1 deals with the background of the proposed problem and seismic interferometry. It also contains the objectives of the study, motivation, and gains of the study upon successful completion.

Chapter 2 gives general overview of relevant previous works on historical development of seismic interferometry and relevant previous studies on supervirtual seismic

interferometry.

Chapter 3 outlines the basic theory of supervirtual seismic refraction interferometry and the comprehensive detail on how 3D synthetic data used in this study is generated. The basic theory is discussed sequentially with relevant equations to illustrate the supervirtual algorithm. Details of the supervirtual methods namely: Crosscorrelation; Alignment; Summation; and First-arrival calculation are also discussed in this chapter.

Chapter 4 consists of a general overview of results presentation and sequential results discussion of the supervirtual algorithm. Also in this chapter, the 2 layer velocity model and the 3D seismic refraction acquisition geometry used in this study are described in detail. The chapter also contains the results of synthetic 3D seismic refraction data generation and enhanced traces after performing the supervirtual algorithm. Also, there is a discussion on supervirtual algorithm whereby first-arrival calculation was used to bring the enhanced trace to its correct time. Finally, results are analyzed in the form of tables and plots, and their outcomes are presented and discussed in this chapter.

In **Chapter 5**, conclusions are drawn based on the 3D seismic refraction supervirtual algorithm results and some recommendations are suggested for further studies.

CHAPTER 2

LITERATURE REVIEW

2.1 General Overview

In this chapter, we discuss the general overview, some applications, previous studies of seismic interferometry, and then narrow down to some previous works relating to supervirtual seismic refraction interferometry.

Fundamentally, seismic refraction interferometry comprises of crosscorrelation of trace pairs and stacking the resulting crosscorrelelograms to generate virtual traces (Schuster, 2009b), similar to raw seismic traces. In terms of source and receivers pairs during data acquisition, apparently, the source has been redatumed close to the receiver after crosscorrelation which produces high amplitude at a particular time lag applied to the trace pairs.

Previous studies applied this method to image the subsurface and solve some seismic wave propagation and interface effect problems. For instance, Miyazawa et al. (2008) use seismic interferometry to extract longitudinal and shear waves from the incoherent

noise source. This method is also used by Nicolson et al. (2012) to extract meaningful information about the subsurface from noisy seismic data. Seismic interferometry is also used to improve SNR and enhance data quality of near-surface seismic data (Ji-Xiang, 2014; Al-Shuhail, 2015). Due to the progress made in the applications of seismic interferometry, it is important to discuss this overview with respect to its historical development.

2.2 Previous Studies of Seismic Interferometry

Claerbout (1968) showed that crosscorrelation of seismic trace recorded from an energy source that have traveled down to a deeper reflector and come back to the same point on the Earth surface with itself, could reconstruct the Green's function between the reflector and the Earth's surface. Claerbout's speculated that this process could work for three-dimensional Earth, which remained unestablished for over two decades. Duvall et al. (1993) proved that solar surface noise at a geometrical pattern could be crosscorrelated to deduce time-distance seismograms. This was the first attempt to prove Claerbout's speculations; however, it was demonstrated using solar data. Rickett and Claerbout (1999) worked on helioseismology and proved that crosscorrelation of noisy seismic traces obtained from receivers at two different positions on the Earth surface, could yield the seismic signal recorded at one of the locations and another signal at the second location behaving as if it was a seismic source. Lobkis and Weaver (2001) proved the methods by demonstrating an experiment in the laboratory. Wapenaar (2003), Wapenaar (2004), and Wapenaar and Fokkema (2006) formulated math-

ematical equation for dealing with elastic media which simulate real field data. van Manen et al. (2006) formulated mathematical equation for acoustic media. Dong et al. (2006) showed that crosscorrelation of two traces A and B recorded at different locations on the Earth surface could yield a virtual trace that has a virtual refraction arrival time. Replicating the process for any post-critical source location yields virtual trace of the same virtual refraction travel time. Mallinson et al. (2011) introduced crosscorrelation and convolution methods to expand the regulator of seismic refraction study by reproducing supervirtual traces with better SNR than the actual traces. Lin et al. (2012) used ambient noise correlation with a dense 3D survey conducted in Long Beach, California, to estimate subsurface velocity. They showed that both Rayleigh wave and body wave signals can be clearly observed in the 0.2-10 Hz frequency range in the noise crosscorrelation. The observed signals also compare well with an active source gather. Mikesell et al. (2012) developed a “modified delay-time method,” wherein they estimate receiver-side delay times and isolate the arrival times of the virtual refraction. They observed that virtual refraction is a spurious arrival found in wave fields estimated by seismic interferometry. Their method removes the source term from the delay-time equation. It is more robust in the presence of noise, and extends the lateral aperture compared to the conventional delay-time method. Their algorithm was tested with an elastic 2D numerical example, where they estimated the receiver delay-times above a horizontal refractor. Taking advantage of reciprocity of the wave equation and rearranging the common shot gathers into common receiver gathers, it was shown that isolated source delay times could also be obtained. Al-Shuhail et al. (2013) used seismic inter-

ferometry to enhance passive seismic events. Their methods include crosscorrelation of seismic traces recorded at reference receiver location with traces recorded at other receiver locations. Next step is the alignment of the crosscorrelation traces to zero timing by applying shifts that correspond to the maximum crosscorrelation value. The aligned crosscorrelation traces are summed to yield stacked traces with better SNR than the individual correlograms. Lastly, the stacked traces were convolved with raw traces to put the enhanced traces at their correct timing. The result shows an improved first arrival of passive seismic events. Quiros et al. (2014) reported the results of two experiments designed to evaluate the utility of cultural noise, as opposed to natural noise as a source for generating virtual body waves via interferometry. They proposed that cultural noise caused by vehicular movement, could effectively produce P and S waves at frequencies and amplitudes applicable for seismic imaging. Therefore, such noise could be considered a signal when using seismic interferometry method. Al-Shuhail (2015) used supervirtual seismic interferometry method to improve automatic picking of first arrivals in active seismic data. The method was tested on 2-D synthetic and real petroleum seismic data.

2.3 Previous Studies of Supervirtual Method

This method enhances first arrivals and improves the SNR of seismic refraction data (Al-Shuhail, 2015). The method of seismic interferometry usually increases SNR by a factor of \sqrt{N} for N numbers of sources. However, if the supervirtual algorithm is applied, the SNR could improve up to a factor of N (Hanafy and Al-Hagan, 2012).

Bharadwaj et al. (2013) apply the supervirtual interferometry method to enhance first arrivals of far offset ocean bottom seismic (OBS) data, which increases the number of pickable arrival times. This extends the coverage area of the survey by preserving far offset arrivals that would have been rendered useless due to bad traces. It is, however, important to note that the far offset arrivals might not come from first subsurface refractor but may come from deeper seismic refraction interfaces.

Generating supervirtual traces comprises of two principal stages (Alshuhail et al., 2012). The first stage involves crosscorrelation of traces recorded from postcritical sources to generate virtual traces, and the second stage is the convolution of the virtual traces with the raw traces (i.e traces before crosscorrelation) to create the supervirtual traces (Bharadwaj et al., 2012). However, the process of convolving the enhanced traces with the raw traces re-introduces certain proportion of noise back into the data by generating side lobes (Alshuhail et al., 2012) around the maximum amplitude of the enhanced traces. To fix this problem, we proposed a semi-automatic first-arrival calculation method which is discussed in detail in chapter three.

Lateral inhomogeneity is a major challenge in extending the supervirtual interferometry method from 2D to 3D. It is pertinent to consider the area extent of the subsurface refractor which may not be as wide as the coverage area of the 3D acquisition design commonly used in the petroleum industry. However, if the 3D acquisition design accommodates a huge amount of sources and receivers (Alshuhail et al., 2012) in a single patch, this challenge could be overcome. Furthermore, we assume that the refracted rays follow the same ray paths in 2D supervirtual interferometry (SVI), however, this

concept does not apply to the 3D SVI. The process of integration of sources and receivers pairs adequately takes care of the ray path problem in 3D SVI (Lu et al., 2014). This was properly taken into account in this study and its concept was used to generate our 3D code for the 3D supervirtual refraction algorithm.

CHAPTER 3

METHODOLOGY

3.1 Theory

The seismic signal recorded during refraction surveying is known as the head wave. When the refracted angle of incidence is greater than the angle at which the refracted signal travels at the interface between low and high-velocity layers, a head wave will occur. Head wave is refracted back to receiver in the upper layer at an angle equal to the critical angle (Figure 3.1).

In a simple seismic refraction acquisition model where velocity increases with depth, the head wave (Figure 3.2) which is our focus in this study, propagates along the subsurface refractor which occur at the interface between low-velocity and high-velocity media. The head wave arrivals from each geophone can have approximated in Fourier domain (Mallinson et al., 2011). The mathematical expressions below for the arrivals and crosscorrelation are summarized from Mallinson et al. (2011), Dong et al. (2006) and Schuster (2009a). Given the head wave arrival times from source to subsurface

refractor beneath the first and second receivers respectively, arrivals equations are described as follows.

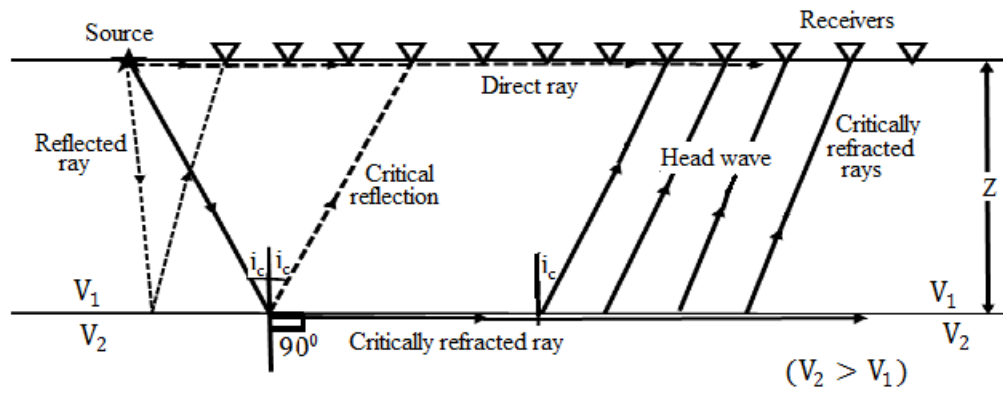


Figure 3.1: Schematic diagram showing reflected ray, direct ray and the critically re-fracted rays which also known as the head wave.

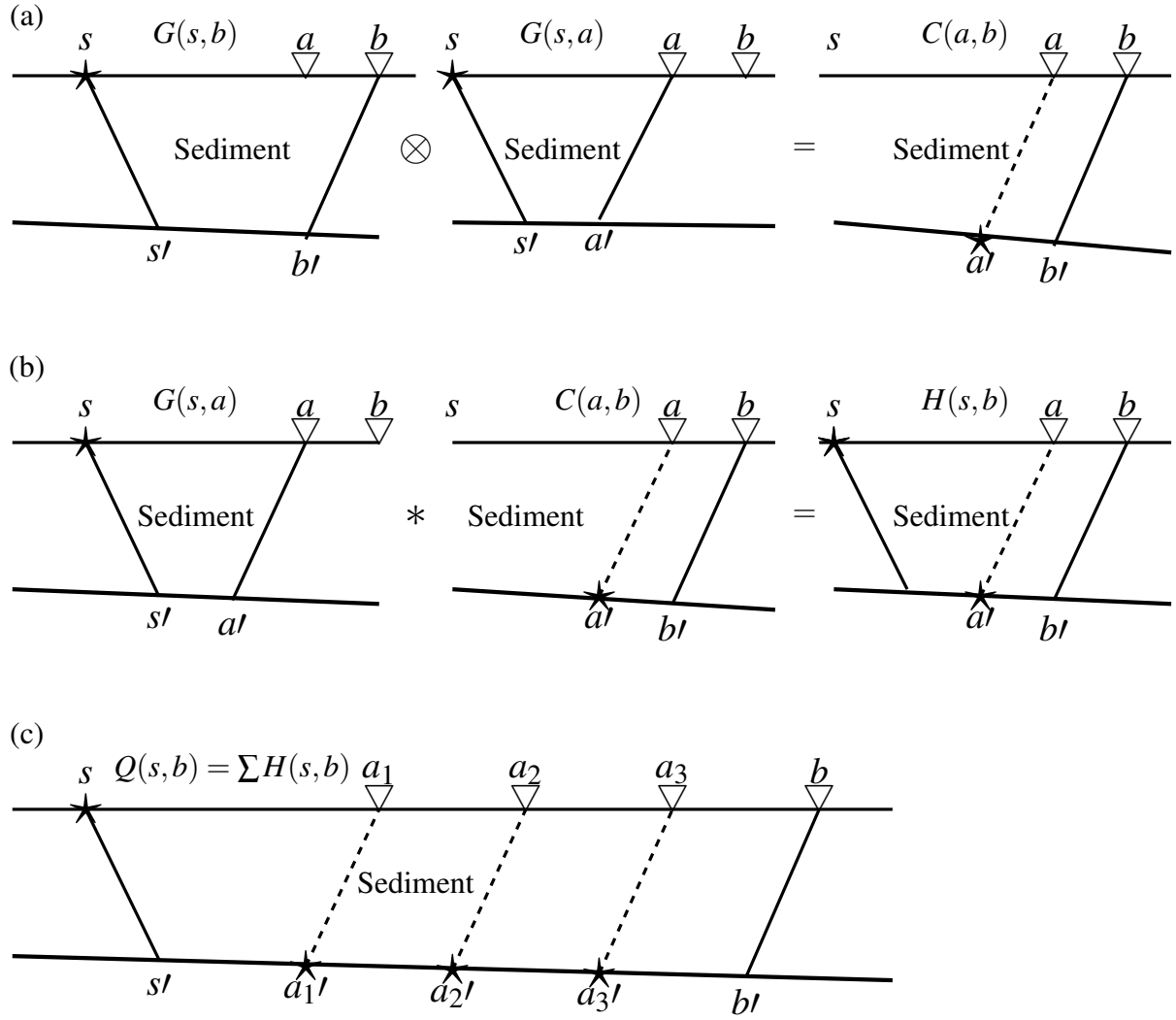


Figure 3.2: Schematic Diagram of Supervirtual Traces: (a) Crosscorrelation; (b) Con-
volution; (c) Summation.

The head wave arrival at the first receiver position ($G(s,b)$) is given by:

$$G(s,b) = A(s,b)e^{i\omega(\tau_{sa'} + \tau_{a'b})} \quad (3.1)$$

and the head wave arrival at the second receiver position ($G(s,a)$) is given by:

$$G(s,a) = A(s,a)e^{i\omega(\tau_{sa'} + \tau_{a'a})} \quad (3.2)$$

where $A(s,b)$ and $A(s,a)$ are the amplitude term for first and second receiver locations respectively, s is the source position, a and b are the receiver positions, $\tau_{sa'}$ is the travel time from s to a' , $\tau_{a'b}$ is the travel time from a' to b and $\tau_{a'a}$ is the travel time from a' to a . To generate virtual refraction, we crosscorrelate the two traces from each receivers (i.e. trace a with trace b), which redatum the source to a point on the subsurface refractor beneath the first receiver location (Dong et al., 2006; Schuster and Zhou, 2006). The seismic signal is induced at an early time describe in Figure 3.2. The mathematical relations for the crosscorrelation of trace a with trace b is shown below:

$$C(a,b)_s = G(s,b) \otimes G(s,a) \quad (3.3)$$

$$= |A(s,a)| |A(s,b)| e^{i\omega(\tau_{sa'} + \tau_{a'b} - \tau_{sa'} - \tau_{a'a})} \quad (3.4)$$

$$\approx |A(s,a)|^2 e^{i\omega(\tau_{a'b} - \tau_{a'a})} \quad (3.5)$$

where $C(a,b)_s$ is the crosscorrelation term of traces at receiver positions a and b due to source s . The factor $(\tau_{a'b} - \tau_{a'a})$ describe the difference in arrival time of traces

recorded at locations a and b. In the above equation, amplitude terms from the two traces are assumed to be the same and are independent of receiver locations. Therefore, we conclude that the crosscorrelation of two different traces (recorded at point a and b) with each other, generates an event similar to an event recorded when the source is placed at the subsurface refractor beneath the first receiver which is at the divergence point. The source of this event has an early time of $\tau_{a'a}$ and it is not depending on the main source location, as long as the subsurface refractor's offset is postcritical. If we crosscorrelate these two traces from many sources and generate a common-pair correlogram of a N number of trace cross-correlations, we may sum them up to obtain an enhanced correlogram with better SNR. Therefore the equation for the enhanced correlogram ($E(a, b)$) can be written as follows:

$$E(a, b) = \sum_{s=1}^N C(a, b)_s \quad (3.6)$$

$$\approx \sum_{s=1}^N |A(s, a)|^2 e^{i\omega(\tau_{a'b} - \tau_{a'a})} \quad (3.7)$$

The above equation describes the trace recorded at b, with ray-path from source position on the subsurface refractor at point a' with refraction source time of $-\tau_{a'a}$. Notice that the equation is particular with waves that obey head wave assumptions, all other waves recorded by the receivers, such as primary, ground roll and multiples will experience destructive interference while the head wave will experience constructive interference (Mallinson et al., 2011) when crosscorrelated and summed together.

The time effect of crosscorrelation and summation shows that the arrival times of the raw traces have been shifted to arrival times of the enhance traces, due to the problem

associated with early time initiation of repositioning the source. Hence, there is a need to bring the enhance traces back to their correct time. To achieve this, we convolve the virtual traces with the raw traces which will generate supervirtual refraction traces because it appears the source has been repositioned back to a new position at the surface as shown in Figure 3.2. The equation for describing this scenario is shown below:

$$H(s, b) = G(s, a) * E(a, b) \quad (3.8)$$

$$= A(s, a) e^{i\omega(\tau_{sa'} + \tau_{a'b})} \sum_{s=1}^N |A(s, a)|^2 e^{i\omega(\tau_{a'b} - \tau_{a'a})} \quad (3.9)$$

$$= A(s, a) \sum_{s=1}^N |A(s, a)|^2 e^{i\omega(\tau_{sa'} + \tau_{a'b})} \quad (3.10)$$

Equation 3.10 describes the trace recorded at the receiver position b , with the source position s . This generated trace $H(s, b)$ is known as supervirtual trace and its travel time is described by factor $\tau_{sa'} + \tau_{a'b}$ as shown in the above equation. The supervirtual equation shows that at far offset ($\tau_{sa'} + \tau_{a'b}$), high amplitude ($|A(s, a)|^2$) can be obtained. Repeating this procedure for all R number of traces and consideration of all source-receiver pairs from the same subsurface refractor will generate many traces and when stacked will increase SNR of the raw traces by \sqrt{R} . The equation describing the receiver stacking process is as shown below:

$$Q(s, b) = \sum_{r=1}^R H(s, b)_r \quad (3.11)$$

$$= \sum_{r=1}^R A(s, a) \sum_{s=1}^N |A(s, a)|^2 e^{i\omega(\tau_{sa'} + \tau_{a'b})} \quad (3.12)$$

$Q(s,b)$ described the supervirtual traces summed together to generate enhanced traces with better SNR, r and s depicts the receivers and sources respectively, where N is the number of sources and R is the number of postcritical head wave traces recorded. As the offset increases, the value of R also increases, so it is offset dependent. This practically solves the problem of low SNR recorded at far offset in the raw traces, because the supervirtual traces SNR increases with offset. This entire process can be replicated for several receiver lines to form a 3D grid, as described in detail later. It is pertinent to note that convolving the enhanced trace with the raw trace will re-introduce noise into the data, as a result, the initial source wavelet is no longer preserved. Side lobes are formed around the main wavelet after convolution which distorts the first arrival wave shape and poses a great challenge during picking (Alshuhail et al., 2012). To overcome this problem we consider a semi-automatic method to shift back the first-arrival on the enhanced trace to its correct time. The semi-automatic method is discussed in detail in a later section.

3.2 Synthetic 3D Seismic Refraction

3.2.1 Synthetic 3D Seismic Refraction Description

In this research work, I use synthetic 3D seismic data with acquisition geometry based on predetermined sets of parameters. To make the 3D acquisition geometry easily adaptive to supervirtual algorithm, we decided to use single patch orthogonal field layout (Figure 3.3) with the following acquisition parameters;

1. Receiver lines laid parallel to each other.
2. Source lines laid parallel in a direction orthogonal to receiver lines.
3. An area of receivers (patch) considered appropriate for this study which has 5 receiver lines with 21 receivers each, 50m source interval, 50m receiver interval, 250m source line interval and 250m receiver line interval.

The acquisition is similar to active 3D seismic land acquisition procedure. Firstly, sources within the patch area are shot and recorded by each of the receivers. In this case, all the 105 receivers will record signal from the same source as shown in Figure 3.3. Sources on the same source line (going inside the patch) are detonated (synthetically) and recorded by the same patch, the procedure will continue until all sources (105) within the patch are detonated. The records are therefore separated into shot gathers and receiver gathers, preparing the data for the processes of crosscorrelation, aligning, summation and shifting of the enhanced traces to their correct positions.

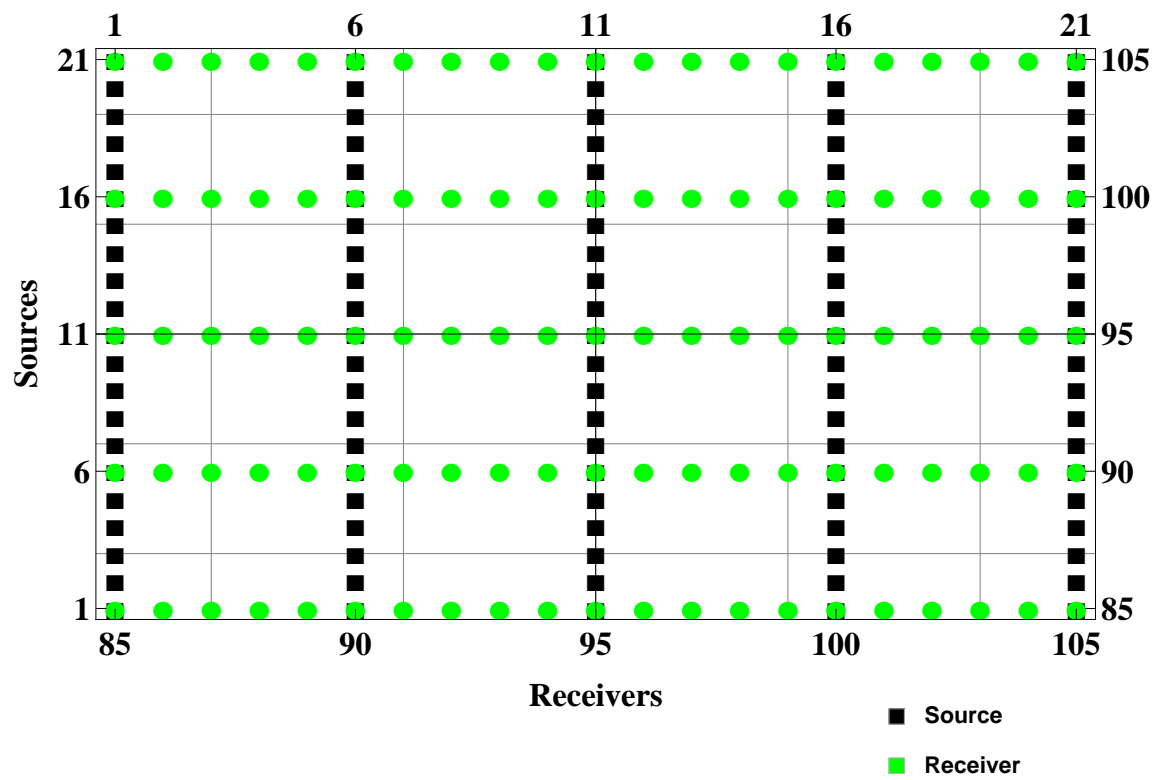


Figure 3.3: 3D layout used to generate synthetic data

3.2.2 Synthetic 3D seismic refraction data generation

The synthetic data used in this project is generated by convolving a zero phase wavelet with refraction travel time computed using seismic refraction arrival time equation.

Source wavelet is computed using the equation below:

$$S_w = e^{-(\pi ft)^2} - (\pi ft)^2 e^{-(\pi ft)^2} \quad (3.13)$$

where S_w is the source wavelet, f is the dominant frequency and t is the time. Using the frequency of 25Hz, source wavelet is computed for t ranging from $-w$ to w , where $w = 1/f$ (Figure 3.4).

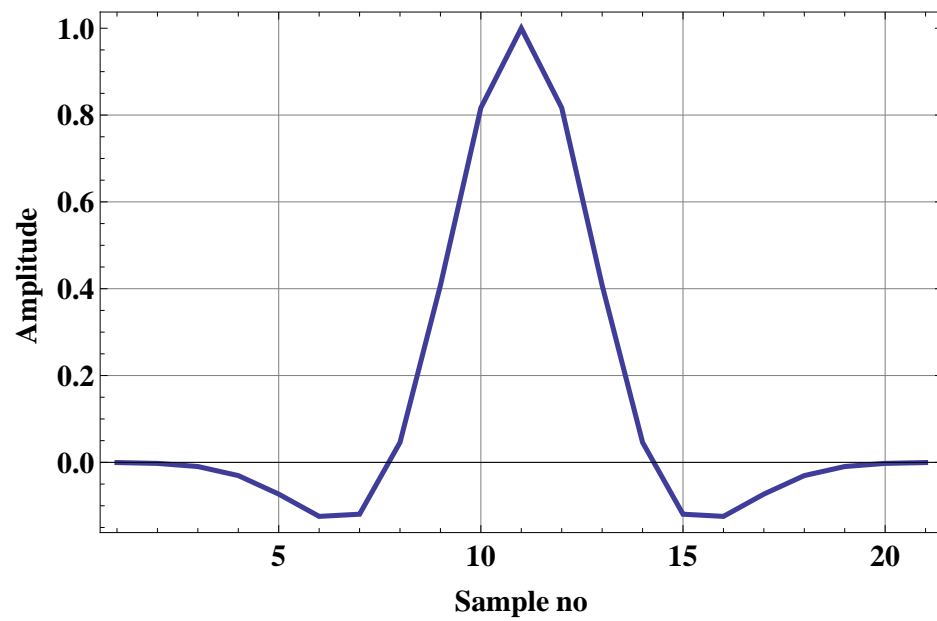


Figure 3.4: Zero phase wavelet

The refraction arrival is computed as follows:

$$t_a = \frac{2h}{V_1} \frac{\sqrt{V_2^2 - V_1^2}}{V_2} + \frac{x}{V_2} \quad (3.14)$$

where h is the depth from the surface to the refractor, V_1 and V_2 are the upper and lower layer velocities respectively, x is the offset.

The single patch orthogonal geometry used in this study consists of 5 receiver lines and 5 source lines. Each source line has 21 sources and each receiver line has 21 receivers. A simple two-layer model ($V_1 = 1500m/s, V_2 = 2500m/s$) is adopted here. Figure 3.5 shows the 3D velocity model and the arrays of sources and receivers. The data are recorded per source because records from the same source assume to have a similar signal. The data are then separated into shot gathers per receiver line.

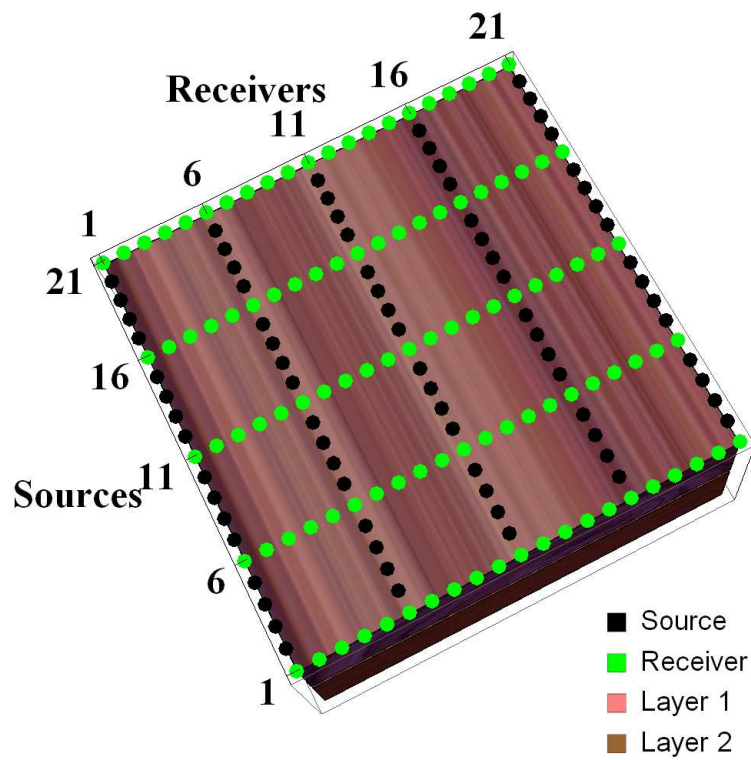


Figure 3.5: 3D sources and receivers layout for 2 layer case

3.3 The 3D Supervirtual Seismic Refraction Interferometry Method

The supervirtual algorithm used in this study is adapted from Al-Shuhail et al. (2013) and Al-Shuhail (2015) and its steps are described as follows:

3.3.1 Crosscorrelation

The traces recorded from the same source are crosscorrelated separately. This is because signals from the same source are expected to be similar in all the receivers (Al-Shuhail et al., 2013). For a particular source, trace recorded at the first receiver location is crosscorrelated with traces recorded at the rest of the receiver locations. Similarly, the second proximal trace is correlated with the distal receiver locations. This is done sequentially till the last trace is crosscorrelated. The crosscorrelation process considers two distinct traces at a time and is executed based on receiver lines. That is, all traces from one receiver line are crosscorrelated separately before moving to other receiver lines; this takes care of crossline inhomogeneity of the subsurface refractor. Therefore, all trace combinations are given by:

$$TC = \frac{n(n-1)}{2} \quad (3.15)$$

where TC is the number of trace combinations and n is the number of traces per receiver line. The entire procedure is repeated for all sources and other receiver lines.

Since the traces are from the same source, the enhanced signals are expected to be

similar after crosscorrelation, only note that the time would be different due to different receiver position (Al-Shuhail et al., 2013). This is why the correlograms must be aligned before stacking.

3.3.2 Alignment

This is done to shift the position of the maximum amplitude of each correlogram to common time irrespective of their receiver locations, so that when they are summed up they will add up in phase to create an enhanced signal with better SNR. The timing of a correlogram maximum is given below.

$$t_{ij} = t_j - t_i \quad (\text{for } i = 1, \dots, y-1; \quad j = i+1, \dots, y) \quad (3.16)$$

where t_{ij} is the timing of the correlogram's maximum produced by cross-correlating the i -th and j -th traces, t_i is the first-arrival timing on the i -th traces and t_j is the first-arrival timing on the j -th trace and $y=21$ is the number of traces in a receiver line.

3.3.3 Summation

Summation of the aligned correlograms creates an enhanced trace that has an SNR better than the individual correlograms (Al-Shuhail et al., 2013). The SNR improvement of the stacked correlograms is theoretically equal to $\sqrt{NR * (NR - 1) / 2}$ where NR is the number of cross-correlated receivers. Next, we shift the enhanced trace back to its

correct time.

3.3.4 Semi-Automatic First-Arrival Calculation Method

The Semi-automatic method is used to shift the seismic event back to its correct time. The procedure involves manual picking of the arrival time of one of the raw traces before crosscorrelation. Any raw trace can be used as a reference trace as long as the first arrival can be picked manually. In the synthetic used to test this algorithm, we always consider the picking of first arrival of the first trace since the first arrival can always be picked manually on it. Then we keep this time as an input parameter for semi-automatic algorithm and execute the semi-automatic flow chart as shown in Figure 3.6. After crosscorrelation, alignment and summation, we then use the manually picked arrival time to estimate the correct time for all the traces, which is described in the equation below:

$$t_{me} = t_r + d_{trm} \quad (3.17)$$

$$d_{trm} = t_m - t_r \quad (3.18)$$

where t_{me} is the correct time of first arrival on the $m - th$ enhanced trace, t_r is the first arrival time on the reference (first) trace before crosscorrelation, d_{trm} is the position of the maximum on the correlogram produced by crosscorrelating the $m - th$ trace with the reference trace, and t_m is the first-arrival time on the $m - th$ raw trace.

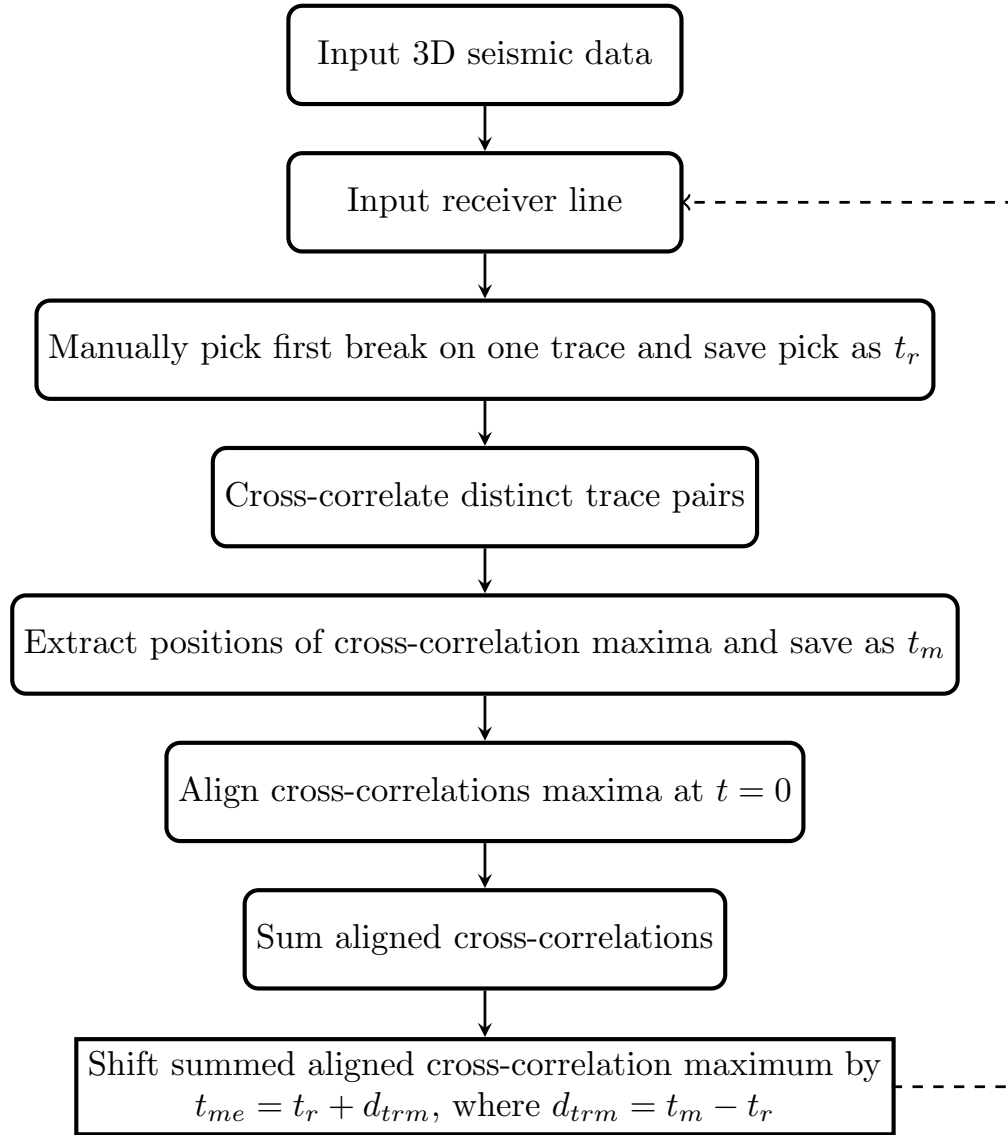


Figure 3.6: Flowchart of 3D Semi-Automatic Method

CHAPTER 4

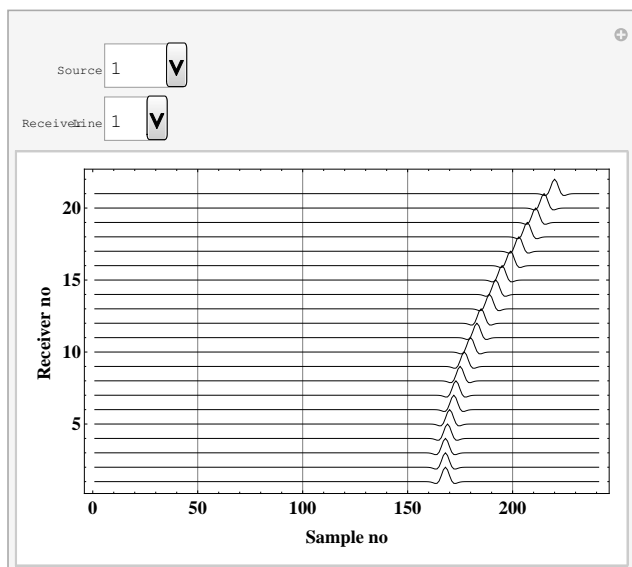
RESULT AND DISCUSSION

4.1 Overview

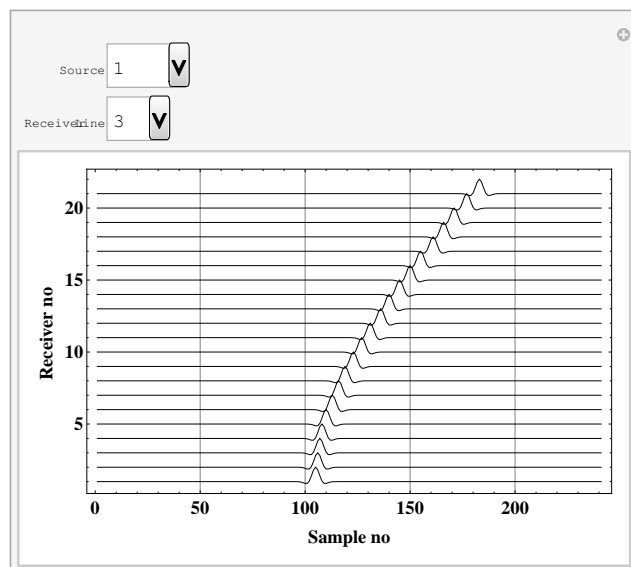
In this chapter, all the results are presented, from the single patch 3D acquisition geometry to the final output of enhanced traces. Results of synthetic seismic refraction generation, supervirtual algorithm, and enhanced traces are presented as wiggle plots. The estimated errors from application of the 3D SVI are presented as linear plots for better comparison. Extracted first arrivals are presented in tabular form while the supervirtual methods are discussed sequentially from crosscorrelation to the semi-automatic method.

4.2 Results of Noiseless 3D Synthetic Seismic Refraction Data

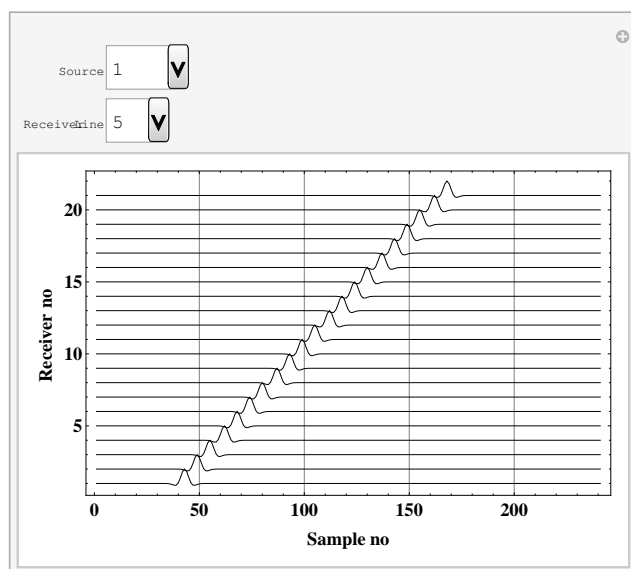
Figures 4.1 to 4.3 show the seismic refraction traces for receiver line 1, 3 and 5, with 21 traces from shot numbers 1, 43, and 105. This is just to show a few of the 3D shots records; any desired shot record could be extracted from the supervirtual computer program. These figures show the trend of the first arrival from different sources. Signals from near sources have the shortest first arrival which signals from far sources have the longest first arrival. Also, trend and shape of first arrivals of these data show the relative position of the sources from the receivers. For instance, figure 4.2c with records from source 43 and receiver line 5, has V-shape first arrival trend. This indicates that source 43 is at the center of the receiver line 5. Also for a straight trend, it indicates that the source is either at the beginning or end of the receiver line, as in the case of figures 4.1c and 4.3a respectively. For later comparison, true first-arrival times are extracted for receiver line 1 from shots number 1, 43, 105 and shown in Table 4.1. These results will be compared with the arrival time after performing the first arrival enhancement algorithm.



(a)

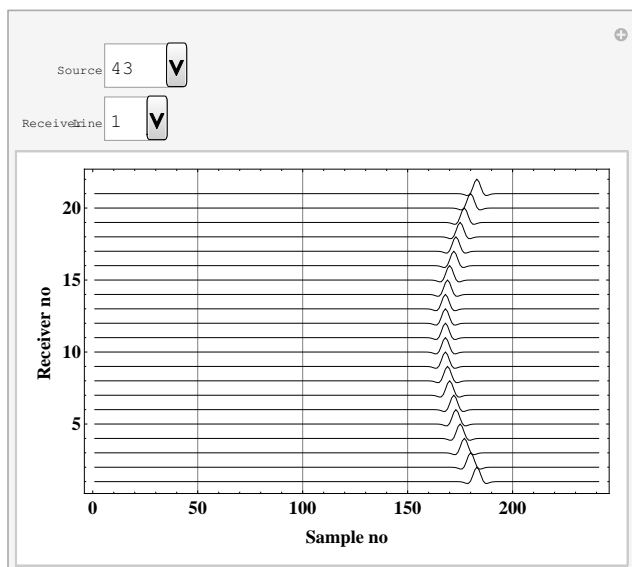


(b)

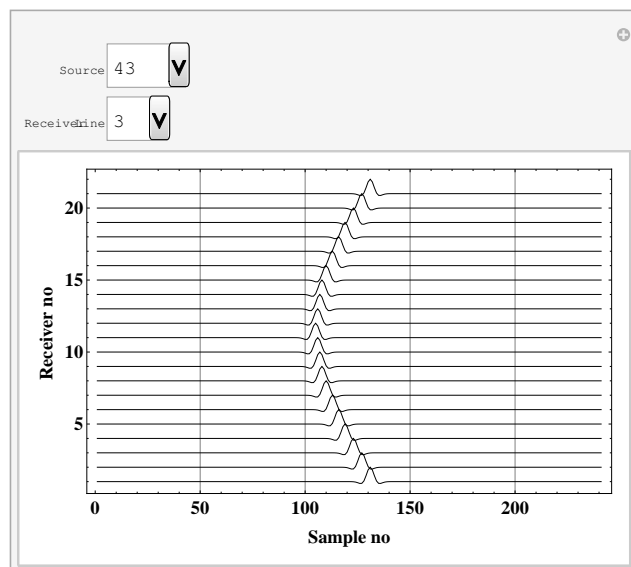


(c)

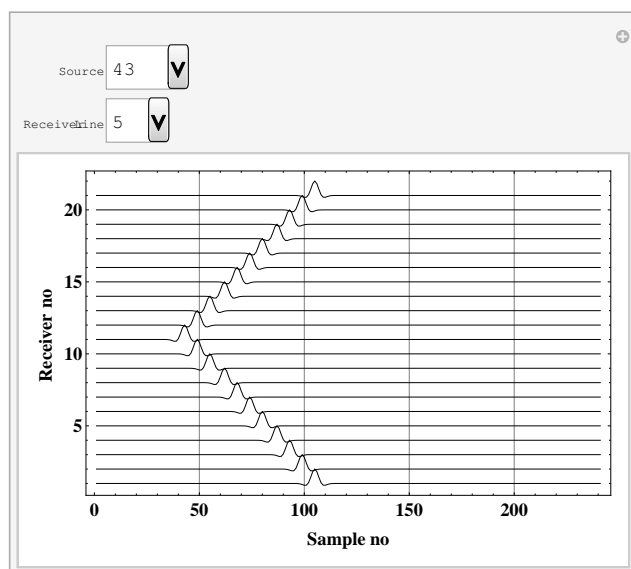
Figure 4.1: Noiseless traces at source 1: (a) receiver line 1; (b) receiver line 3; (c) receiver line 5.



(a)

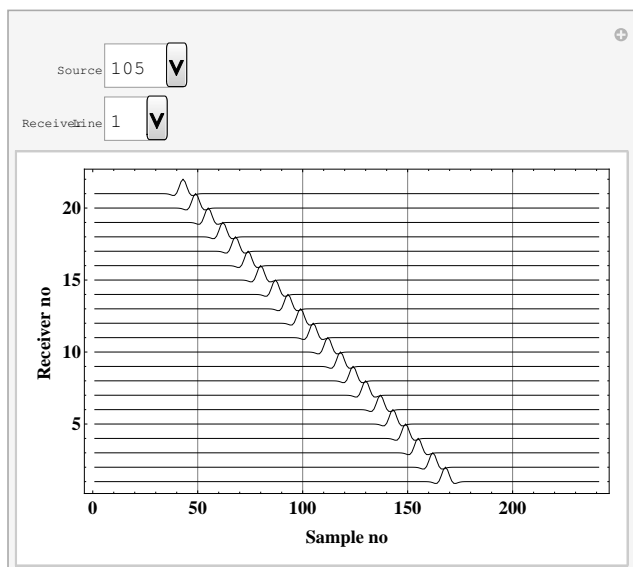


(b)

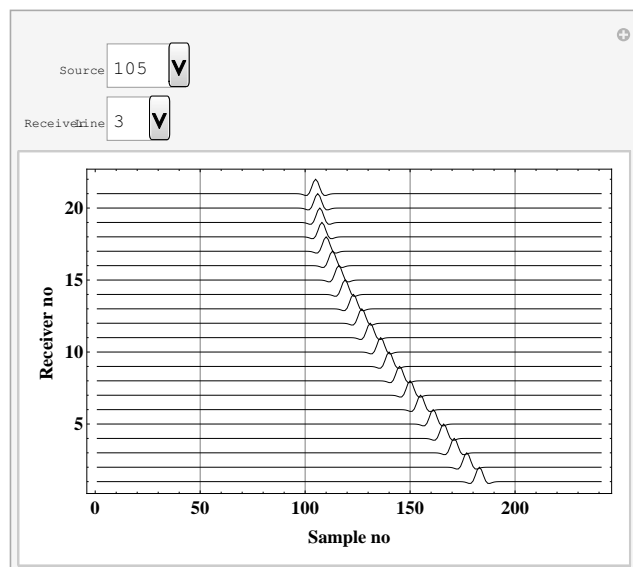


(c)

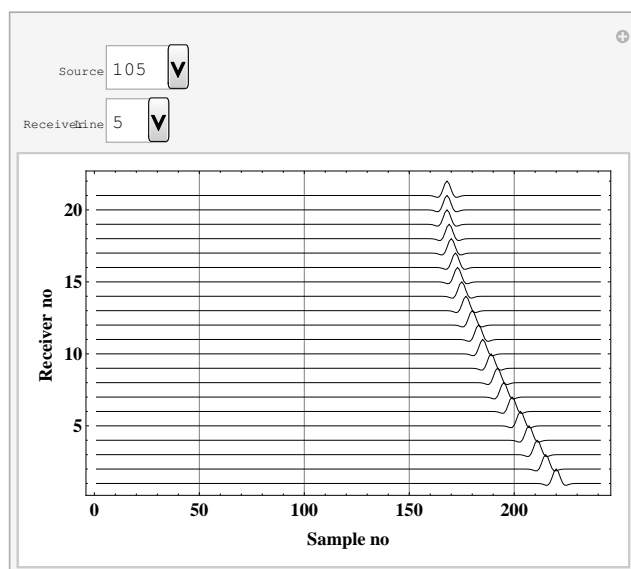
Figure 4.2: Noiseless traces at source 43: (a) receiver line 1; (b) receiver line 3; (c) receiver line 5.



(a)



(b)



(c)

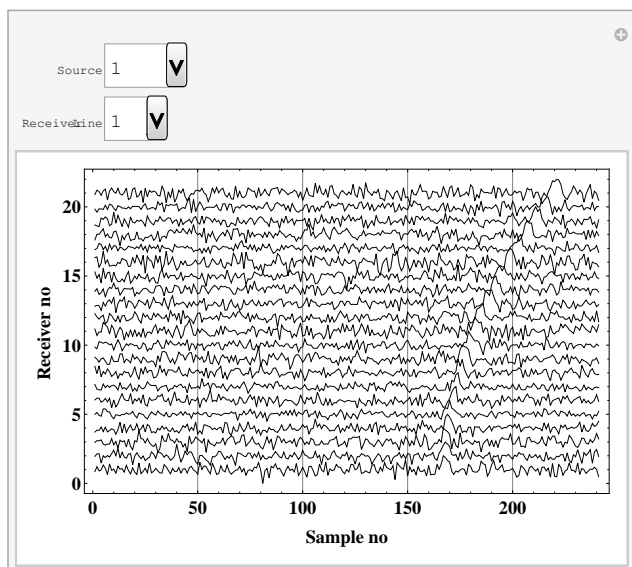
Figure 4.3: Noiseless traces at source 105: (a) receiver line 1; (b) receiver line 3; (c) receiver line 5.

Table 4.1: True first arrivals at all receivers of line 1 from sources 1, 43 and 105

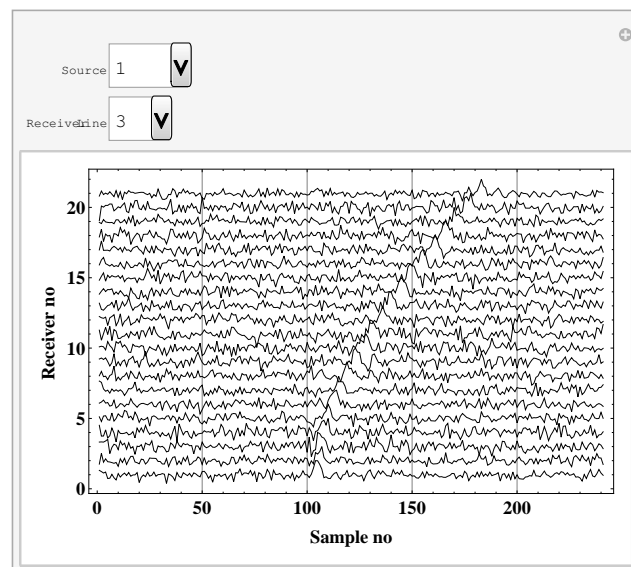
| Receivers | Source 1 | Source 43 | Source 105 |
|-----------|----------------|----------------|----------------|
| | First Arrivals | First Arrivals | First Arrivals |
| 1 | 168 | 183 | 168 |
| 2 | 168 | 180 | 162 |
| 3 | 168 | 177 | 155 |
| 4 | 169 | 175 | 149 |
| 5 | 179 | 173 | 143 |
| 6 | 172 | 172 | 137 |
| 7 | 173 | 170 | 130 |
| 8 | 175 | 169 | 124 |
| 9 | 177 | 168 | 118 |
| 10 | 180 | 168 | 112 |
| 11 | 183 | 168 | 105 |
| 12 | 185 | 168 | 99 |
| 13 | 189 | 168 | 93 |
| 14 | 192 | 169 | 87 |
| 15 | 195 | 170 | 80 |
| 16 | 199 | 172 | 74 |
| 17 | 203 | 173 | 68 |
| 18 | 207 | 175 | 62 |
| 19 | 211 | 177 | 55 |
| 20 | 215 | 180 | 49 |
| 21 | 220 | 183 | 43 |

The above data form the basis of comparison since its parameters are known; results of the supervirtual algorithm are compared for quality control to know if the algorithm gives satisfactory results. This measure boosts our confidence level of the supervirtual methods after passing the quality control test.

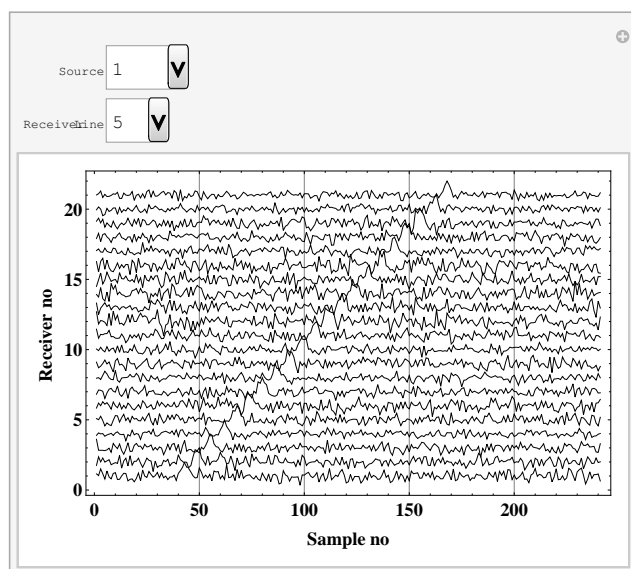
The same amount of Gaussian distribution noise with standard deviation of 0.25 is added to the shot records to make the signal appear imperceptible. Adding this noise level makes the SNR of the noisy traces about 4. The noise level may vary in the real seismic data case, however, the noise level used for this synthetic data is comparable with noisy seismic refraction field records. Although the signal trend may be noticeable in some shot records, automatic first arrival picking at this noise level might be difficult as an interpreter could pick noise arrival time instead of the refraction signal. This is because some of the amplitudes of the noise are equal to that of the signal, in which case, apart from proper and careful signal examination, it may not be easily differentiated around the signal. Therefore to ease first arrival picking and reduce risk associated with mistaking noise for signal in this typical noise level, there is a need for enhancing the first arrival. Figure 4.4 to Figure 4.6 show the shot records after the addition of noise; this simulates typical noisy data in an area with a complex geology problem. Again, the choice to show a few shot records is discretionary, any desired shot record could be extracted from the 3D supervirtual program. Even though the program handles the total sum of the 3D data sequentially, desired shot record could be extracted, this makes the program very robust in handling 3D data.



(a)

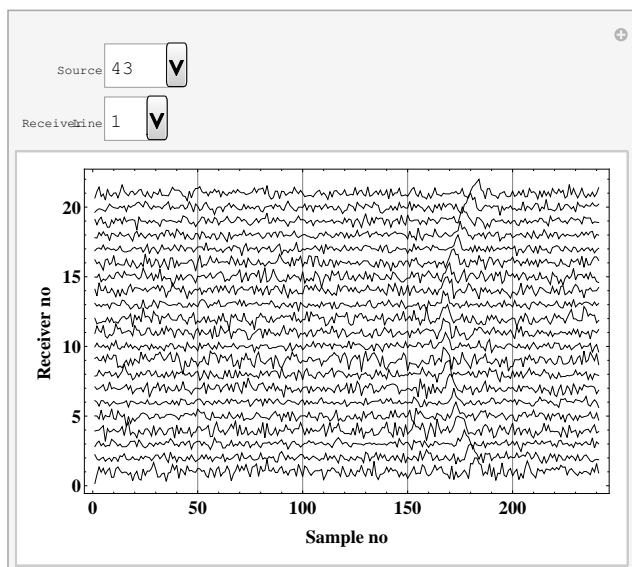


(b)

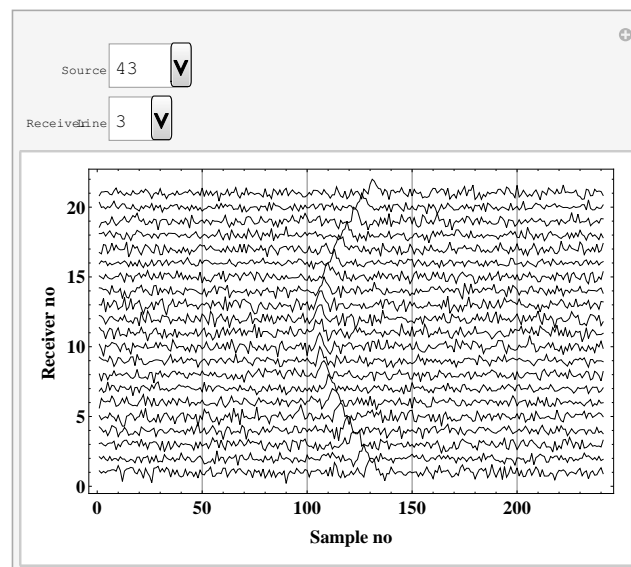


(c)

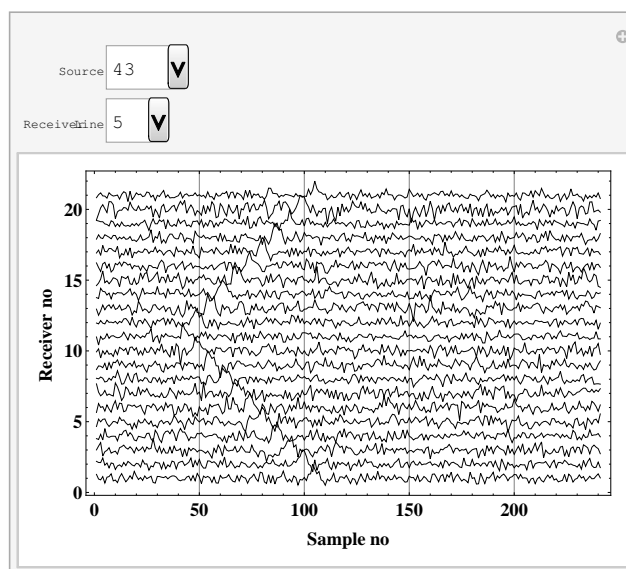
Figure 4.4: Noisy traces at source 1: (a) receiver line 1; (b) receiver line 3; (c) receiver line 5.



(a)

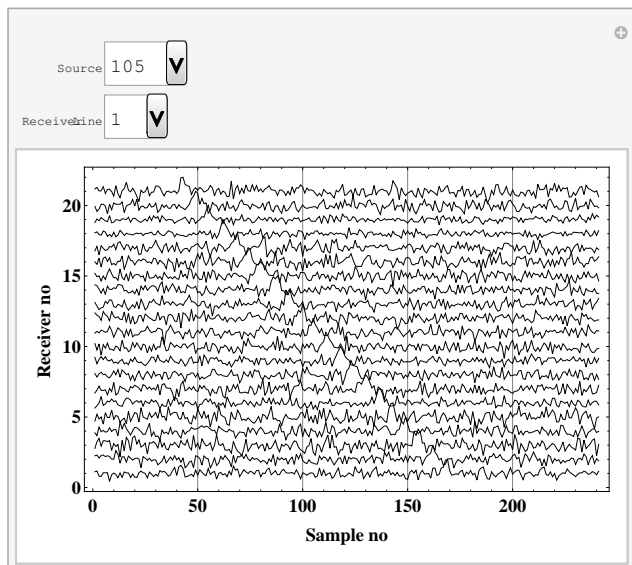


(b)

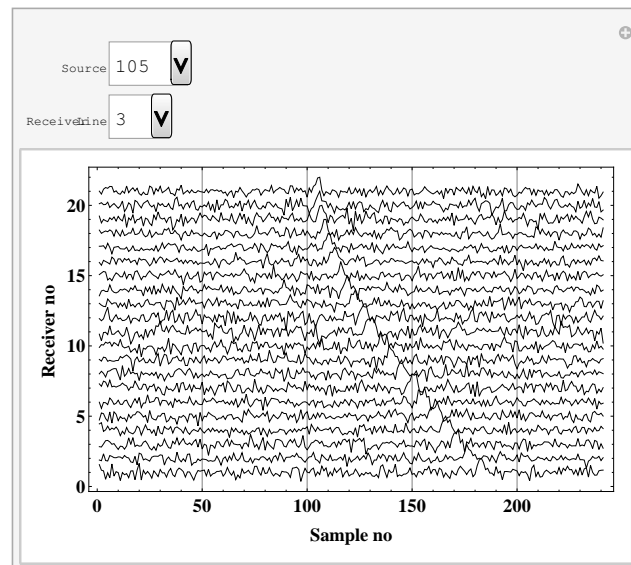


(c)

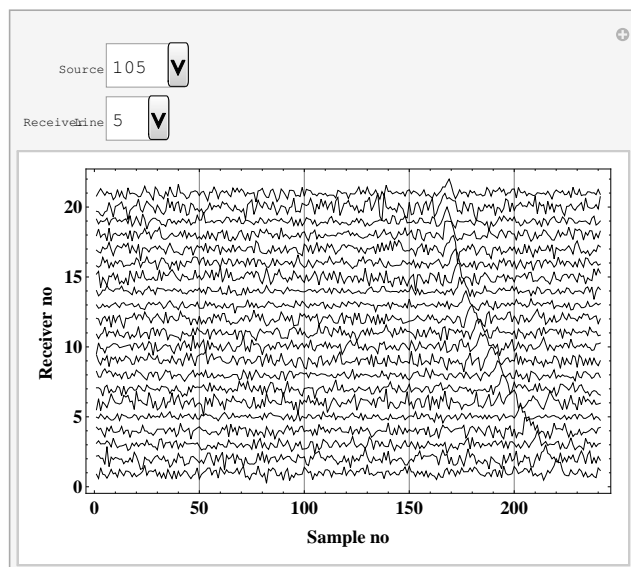
Figure 4.5: Noisy traces at source 43: (a) receiver line 1; (b) receiver line 3; (c) receiver line 5.



(a)



(b)



(c)

Figure 4.6: Noisy traces at source 105: (a) receiver line 1; (b) receiver line 3; (c) receiver line 5.

4.3 Supervirtual Methods

To make the entire shot records adaptive to the supervirtual algorithm, each shot record was separated into receiver lines (inlines). For instance, shot 105, at the first receiver line (line1) has 21 traces, similarly, receiver lines two to five have 21 traces each for the same source position. These traces are crosscorrelated accordingly, beginning with the first receiver line. Using the trace combination techniques discussed in the previous chapter, the result of the crosscorrelation yielded 210 traces per receiver line with a shift in the position of the maximum amplitudes of each of the enhanced traces. This is because the time lag at which the crosscorrelated traces are most similar is not the same as the time of the raw signal before crosscorrelation. Since maximum amplitude is created at time lag where the crosscorrelated traces are most similar, so the maxima positions of the correlograms has to be shifted from its correct time which should be aligned to common time (t_0) so that when they are summed up, they will add up constructively in phase to yield an enhanced signal with better SNR. Figure 4.7 shows the results of crosscorrelation while Figure 4.8 shows the outcome of alignments for the first receiver line from shots number 1, 43 and 105. While most of the maxima positions are aligned to the same time position, a few maxima are not aligned. This could be probably due to the difference between the amplitude of the signal and other correlation sequences. Since we got a substantial amount of the traces that are aligned; we are confident that when summed up it will enhance the signal better.

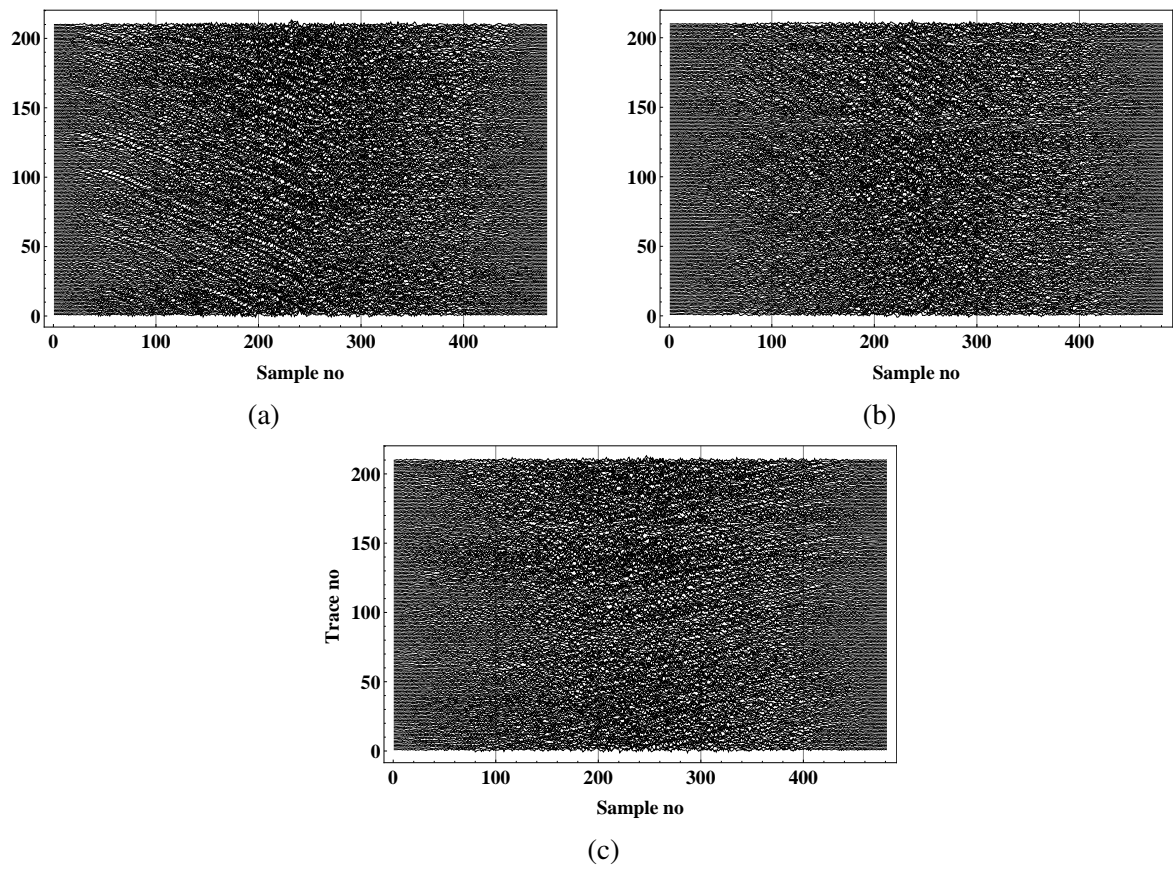


Figure 4.7: Crosscorrelated traces of receiver line 1 from: (a) source 1; (b) source 43; (c) source 105.

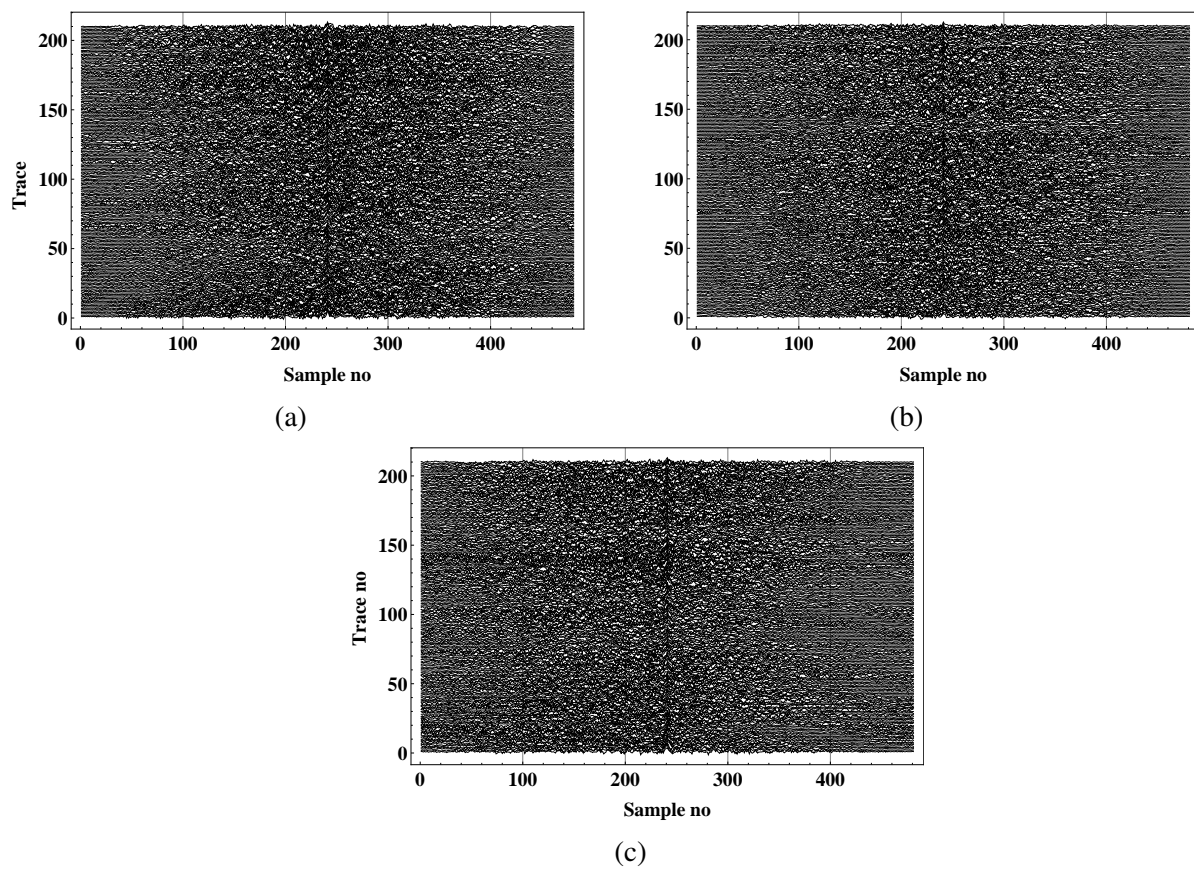


Figure 4.8: Aligned crosscorrelated traces of receiver line 1 from: (a) source 1; (b) source 43; (c) source 105.

Figure 4.9 shows the outcome of the traces after stacking; it shows a clear difference between the noise and the signal. Summation of the correlograms reduced the noise to an average of 0.05 and enhanced the signal to an average of 1 giving a SNR of about 20 compared to a SNR of only 4 for the raw traces. This is a clear improvement of the signal after summation as shown in the Figure 4.9. The virtual traces were shifted to their correct time using the semi-automatic method discussed on the previous chapter. For the first receiver line at shot number 1, the arrival time of the first receiver, $t_{gr1} = 168$ was used. This shows the manually picked time on the first trace within the first receiver line and it is the only stage that is not automated in the proposed algorithm; all other stages are automated. Similarly, $t_{gr2} = 183$, and $t_{gr3} = 163$, are used for receiver line one at shots number 43 and 105 respectively. The procedure was repeated for all the other sources and the outcomes are recorded. Figure 4.10 shows the supervirtual traces after shifting the enhanced traces back to their correct time; it is evident from the result that the noise level is reduced while the signal improves. To visualize how much the traces have been enhanced after the application of the supervirtual methods, noisy traces were plotted alongside enhanced traces and it is clearly shown in Figure 4.11 that the supervirtual algorithm has successfully improved the SNR of the noisy seismic refraction data.

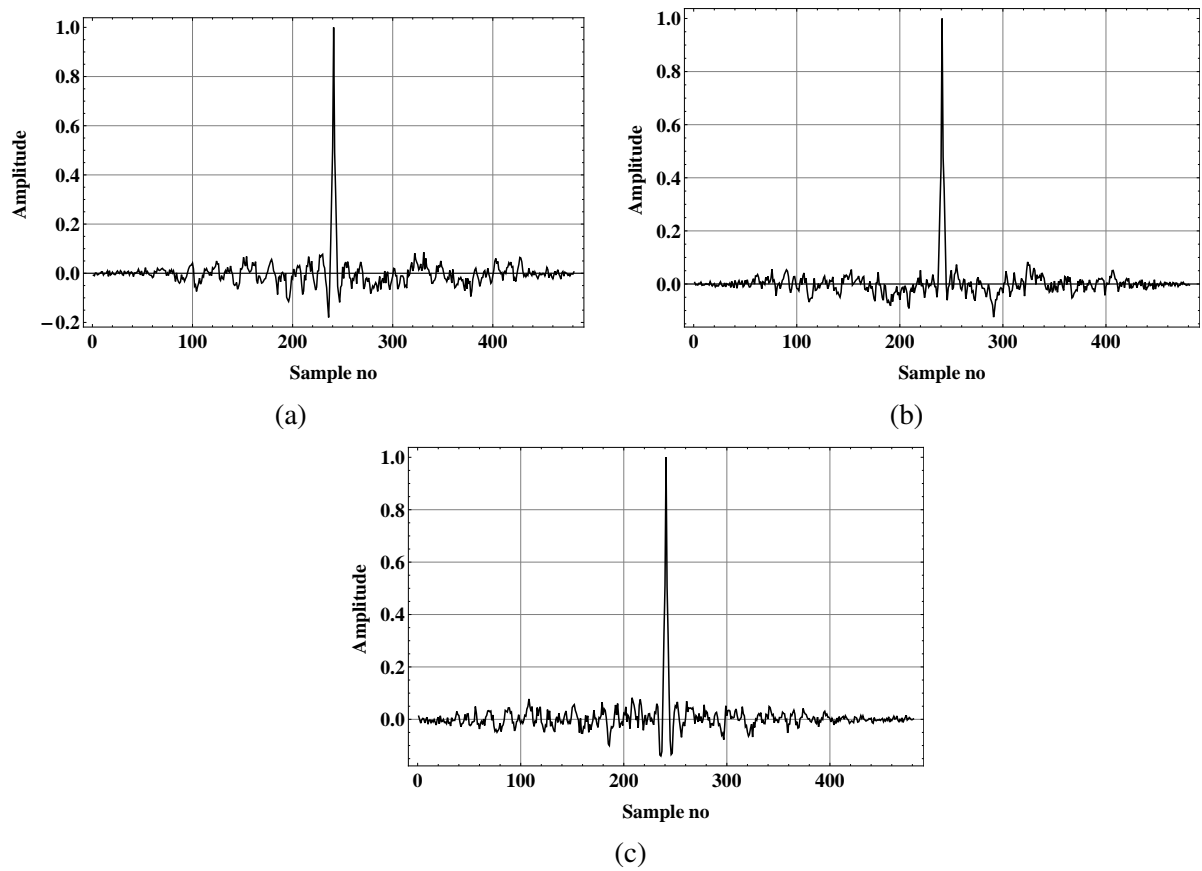


Figure 4.9: Stacked trace of receiver line 1 from: (a) source 1; (b) source 43; (c) source 105.

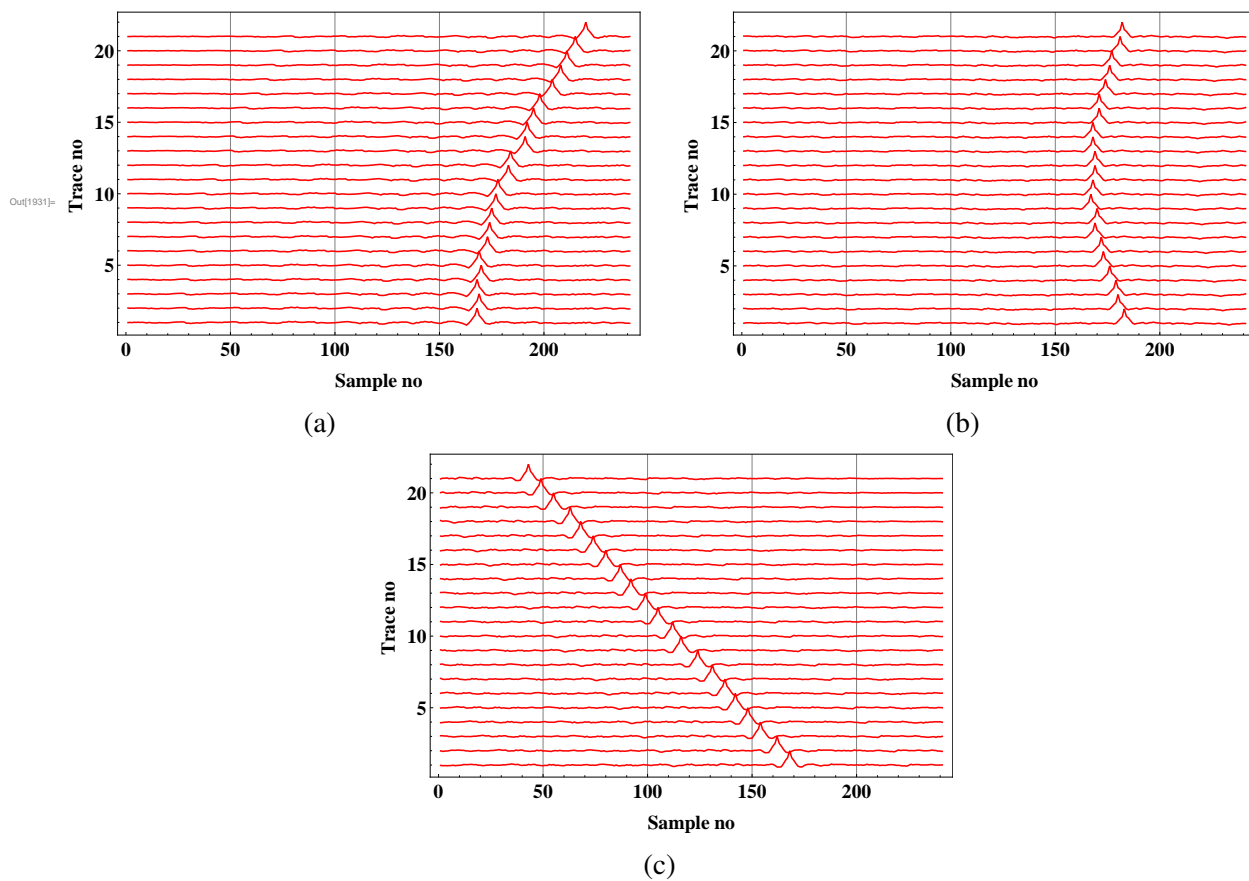
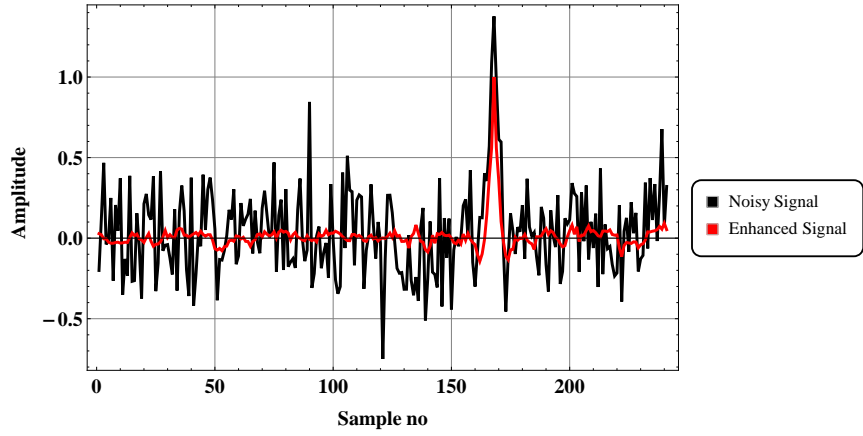
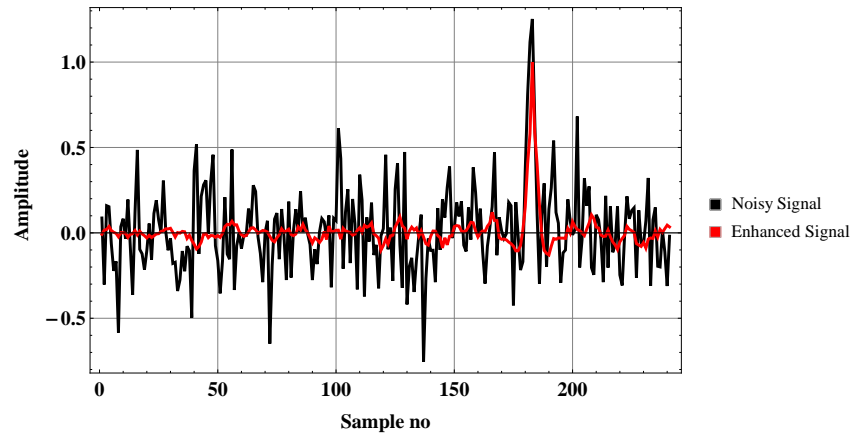


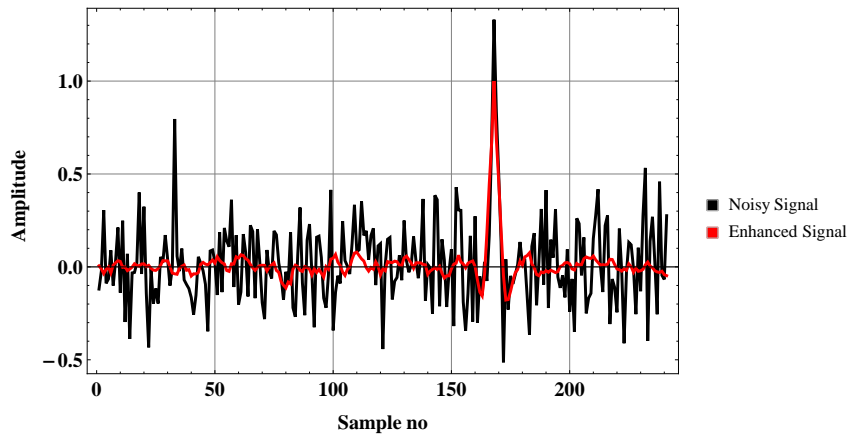
Figure 4.10: Enhanced traces of receiver line 1 from: (a) source 1; (b) source 43; (c) source 105.



(a)



(b)



(c)

Figure 4.11: Amplitude comparison between noisy and enhanced traces of receiver line 1 from: (a) source 1; (b) source 43; (c) source 105.

4.4 Analysis of Results

In order to test the efficiency of the supervirtual algorithm, first arrivals are extracted from the enhanced seismic data after performing the supervirtual methods on the noisy traces and the data are tabulated for comparison. Table 4.2 shows the results of first arrivals from raw traces and after performing supervirtual methods. These first arrivals results were plotted per source (Figure 4.12), and the results show a close match between the noiseless and enhanced traces. Generally, results show first arrivals having a strong correlation with the first arrival of raw synthetic data without noise. Percentage error was computed and plotted, the results show that errors are very small (less than 5%). Visual inspection of the plot of these errors (Figure 4.13) shows the same observation. This makes the proposed method credible in enhancing first arrivals of 3D seismic refraction data.

Table 4.2: Extracted first arrivals from raw synthetic data and after supervirtual method

| Receivers | Source 1 | | Source 43 | | Source 105 | |
|-----------|----------------|-----------|----------------|-----------|----------------|-----------|
| | First Arrivals | | First Arrivals | | First Arrivals | |
| | Noiseless | After SVI | Noiseless | After SVI | Noiseless | After SVI |
| 1 | 168 | 168 | 183 | 183 | 168 | 168 |
| 2 | 168 | 168 | 180 | 180 | 162 | 161 |
| 3 | 168 | 167 | 177 | 177 | 155 | 155 |
| 4 | 169 | 170 | 175 | 173 | 149 | 149 |
| 5 | 170 | 169 | 173 | 172 | 143 | 143 |
| 6 | 172 | 173 | 172 | 173 | 137 | 137 |
| 7 | 173 | 173 | 170 | 170 | 130 | 129 |
| 8 | 175 | 174 | 169 | 168 | 124 | 124 |
| 9 | 177 | 178 | 168 | 170 | 118 | 118 |
| 10 | 180 | 182 | 168 | 169 | 112 | 113 |
| 11 | 183 | 184 | 168 | 168 | 105 | 104 |
| 12 | 185 | 186 | 168 | 167 | 99 | 99 |
| 13 | 189 | 188 | 168 | 168 | 93 | 93 |
| 14 | 192 | 192 | 169 | 167 | 87 | 87 |
| 15 | 195 | 196 | 170 | 170 | 80 | 80 |
| 16 | 199 | 200 | 172 | 172 | 74 | 73 |
| 17 | 203 | 202 | 173 | 171 | 68 | 68 |
| 18 | 207 | 208 | 175 | 177 | 62 | 63 |
| 19 | 211 | 211 | 177 | 177 | 55 | 55 |
| 20 | 215 | 214 | 180 | 180 | 49 | 48 |
| 21 | 220 | 222 | 183 | 182 | 43 | 42 |

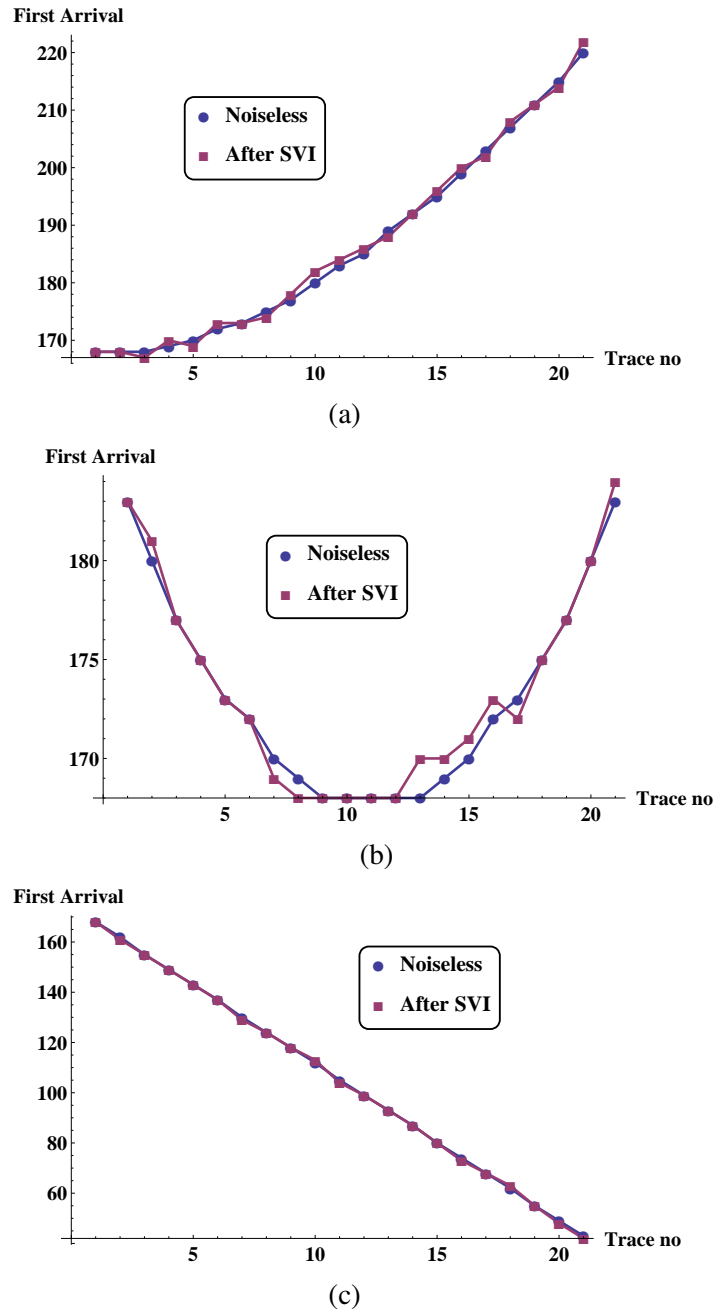


Figure 4.12: First arrival comparison between noiseless traces of receiver line 1 from: (a) source 1; (b) source 43; (c) source 105.

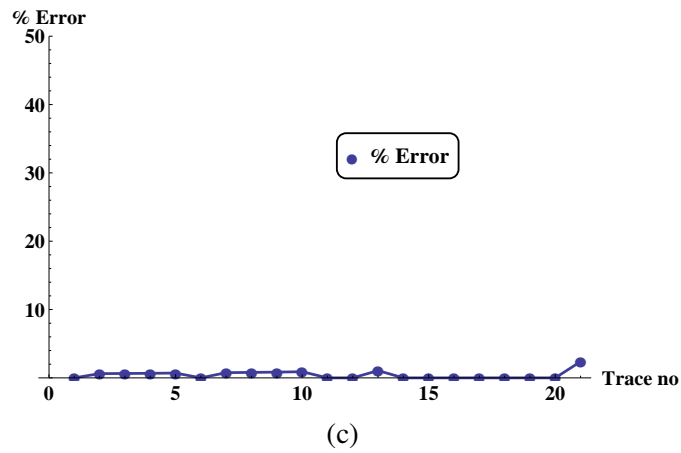
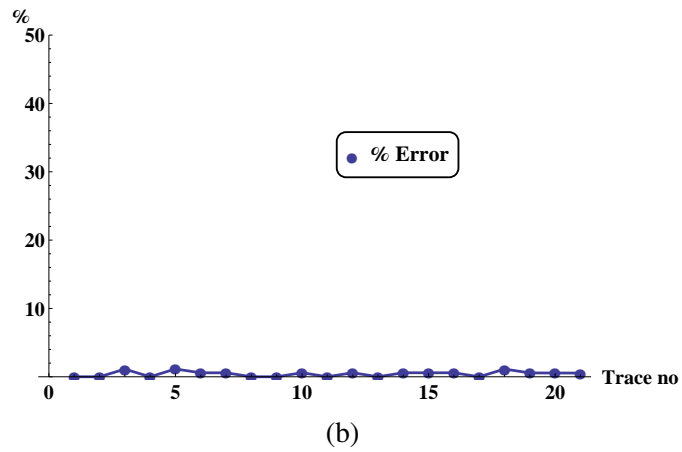
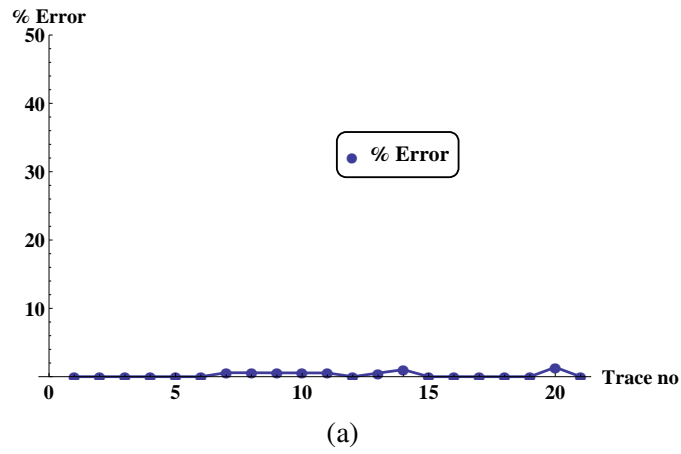


Figure 4.13: Plots of % error against trace numbers of receiver line 1 from: (a) source 1; (b) source 43; (c) source 105.

CHAPTER 5

CONCLUSIONS AND RECOMMENDATIONS

5.1 Conclusions

This thesis demonstrates how supervirtual methods proposed by Al-Shuhail et al. (2013) and Al-Shuhail (2015) could be used to enhance first arrivals of active 3D seismic refraction data. The success of the 3D supervirtual methods is determined by the source and receiver array because subsurface refractor is the main focus of the supervirtual algorithm. Therefore, to image subsurface refractors effectively, the source-receiver array should be decided not too far away. Although the supervirtual method can take care of far offset problems (Mallinson et al., 2011), the geology may not be uniform over the survey area. This study uses a single patch orthogonal array with many sources and receivers which take care of problems associated with inhomogeneity of the subsurface refractors.

Gaussian distribution noise is added to the raw synthetic data to make refraction signal imperceptible. Also for practical analysis, the supervirtual algorithm is performed on each receiver line per shot, because a signal from the same source is expected to be similar at the receiver locations. This procedure is repeated for all the 105 sources in each case performing the supervirtual methods on each receiver line. The outcome shows enhanced signal with first arrival similar to that of the raw synthetic data before the addition of noise which proves the efficacy of the supervirtual methods. The semi-automatic method solves the problem of re-introducing noise into the enhanced traces while trying to shift the signal back to correct time, which is common with the convolution method. This utilizes a reference first arrival pick which could be carried out manually. Aligning all the correlograms to common time makes this algorithm plausible in handling 3D supervirtual interferometry. Generally, most of the errors from the enhancement of traces are less than five percent and some have no error; this shows that the supervirtual method is adequate to enhance first arrivals of active synthetic 3D seismic refraction data.

5.2 Recommendations

The 3D supervirtual algorithm presented in this study is not completely automated. There is need to manually pick the first arrival of the reference trace on each receiver line before performing the semi-automatic method. In the case of handling real seismic refraction data as commonly acquired in the industry, considering the number of traces

that must be manually picked before performing the supervirtual algorithm and its runtime, renders the semi-automatic method inefficient and time-consuming. Therefore, this thesis recommends that the semi-automatic method should be fully automated to cater for this inefficiency in handling large amounts of data.

Also, the synthetic data generated for this study is from a single patch geometry; this should be expanded to many patches, salvos and swath acquisition grids using a high definition computer. That way, the success of the supervirtual methods on the active synthetic 3D seismic refraction data will give clues to how to make it work on the active real 3D seismic refraction data.

Finally, this thesis recommends that this algorithm should be tested using real 3D seismic refraction data.

REFERENCES

- Akram, J., and D. Eaton, 2014, Refinement of arrival-time picks using an iterative, cross-correlation based workflow: Presented at the 76th EAGE Conference and Exhibition 2014.
- Al-Shuhail, A., S. I. Kaka, and M. Jervis, 2013, Enhancement of passive microseismic events using seismic interferometry: *Seismological Research Letters*, **84**, 781–784.
- Al-Shuhail, A. A., 2015, Improving automatic first-arrival picking by supervirtual interferometry: examples from saudi arabia: *Arabian Journal of Geosciences*, 1–10.
- Alshuhail, A., A. Aldawood, and S. Hanafy, 2012, Application of super-virtual seismic refraction interferometry to enhance first arrivals: A case study from Saudi Arabia: *The Leading Edge*, **31**, 34–39.
- Bakulin, A., and R. Calvert, 2004, Virtual source: new method for imaging and 4D below complex overburden: 74th Ann. Internat. Mtg., Soc. of Expl. Geophys., 2477–2480.
- Bharadwaj, P., G. Schuster, I. Mallinson, and W. Dai, 2012, Theory of supervirtual refraction interferometry: *Geophysical Journal International*, **188**, 263–273.
- Bharadwaj, P., X. Wang, G. Schuster, and K. McIntosh, 2013, Increasing the number

- and signal-to-noise ratio of OBS traces with supervirtual refraction interferometry and free-surface multiples: *Geophysical Journal International*, **192**, 1070–1084.
- Claerbout, J. F., 1968, Synthesis of a layered medium from its acoustic transmission response: *Geophysics*, **33**, 264–269.
- Dong, S., J. Sheng, J. T. Schuster, et al., 2006, Theory and practice of refraction interferometry: Presented at the 76th SEG meeting, New Orleans, Louisiana, USA, Expanded Abstracts.
- Duvall, T., S. Jefferies, J. Harvey, and M. Pomerantz, 1993, Time–distance helioseismology: *Nature*, **362**, 430–432.
- Hanafy, S. M., and O. Al-Hagan, 2012, Super-virtual refraction interferometry: an engineering field data example: *Near Surface Geophysics*, **10**, 443–449.
- Kang, T.-S., 2014, Seismic interferometry and ambient noise tomography in east asia: Science reports of Niigata University. (Geology), **29**, 4–5.
- Korneev, V., A. Bakulin, J. Lopez, et al., 2008, Imaging and monitoring with virtual sources on a synthetic 3d data set from the middle east: 78th Annual Meeting, SEG, Expanded Abstracts, 3204–3208.
- Lin, F.-C., D. Li, and R. W. Clayton, 2012, Interferometry with a dense 3D dataset: SEG Technical Program Expanded Abstracts, **82**, 1–6.
- Liu, Y., K. Wapenaar, J. van der Neut, B. Arntsen, et al., 2014, Combining inter-source seismic interferometry and source-receiver interferometry for deep local imaging: Presented at the 2014 SEG Annual Meeting, Society of Exploration Geophysicists.
- Lobkis, O. I., and R. L. Weaver, 2001, On the emergence of the Green’s function in

- the correlations of a diffuse field: *The Journal of the Acoustical Society of America*, **110**, 3011–3017.
- Lu, K., A. AlTheyab, and G. T. Schuster, 2014, 3D supervirtual refraction interferometry, *in* SEG Technical Program Expanded Abstracts 2014: Society of Exploration Geophysicists, 4203–4207.
- Mallinson, I., P. Bharadwaj, G. Schuster, and H. Jakubowicz, 2011, Enhanced refractor imaging by supervirtual interferometry: *The Leading Edge*, **30**, 546–550.
- Mikesell, T. D., K. van Wijk, E. Ruigrok, A. Lamb, and T. E. Blum, 2012, A modified delay-time method for statics estimation with the virtual refraction: *Geophysics*, **77**, A29–A33.
- Nicolson, H., A. Curtis, B. Baptie, and E. Galetti, 2012, Seismic interferometry and ambient noise tomography in the British Isles: *Proceedings of the British Geologists' Association*, **123**, 74–86.
- Nicolson, H. J., 2011, Exploring the Earth's subsurface with virtual seismic sources and receivers: Ph.D. Thesis, University of Edinburgh.
- Quiros, D., L. Brown, and D. Kim, 2014, Seismic interferometry of cultural noise: Body waves extracted from auto and train traffic: *AGU Fall Meeting Abstracts*, 4447.
- Rickett, J., and J. Claerbout, 1999, Acoustic daylight imaging via spectral factorization: *Helioseismology and reservoir monitoring: The leading edge*, **18**, 957–960.
- Schuster, G., 2009a, Finite-Difference Approximation to the Acoustic Wave Equation. Unpublished Lecture Notes, KAUST.
- Schuster, G. T., 2009b, *Seismic interferometry*: Cambridge University Press Cam-

- bridge, **1**.
- Schuster, G. T., and M. Zhou, 2006, A theoretical overview of model-based and correlation-based redatuming methods: *Geophysics*, **71**, SI103–SI110.
- Seimetz, E. X., M. P. Rocha, W. R. Borges, P. V. Nogueira, M. M. Cavalcanti, and P. A. Azevedo, 2013, Integration of geophysical methods to define the geological interfaces for a future metro station located in Brasilia-DF, Brazil: *Geociências* (São Paulo), **32**, 650–658.
- van Manen, D.-J., A. Curtis, and J. O. Robertsson, 2006, Interferometric modeling of wave propagation in inhomogeneous elastic media using time reversal and reciprocity: *Geophysics*, **71**, SI47–SI60.
- Wapenaar, K., 2003, Synthesis of an inhomogeneous medium from its acoustic transmission response: *Geophysics*, **68**, 1756–1759.
- , 2004, Retrieving the elastodynamic Green’s function of an arbitrary inhomogeneous medium by cross correlation: *Physical review letters*, **93**, 254301.
- Wapenaar, K., and J. Fokkema, 2006, Green’s function representations for seismic interferometry: *Geophysics*, **71**, SI33–SI46.

EDIGBUE, Paul Irikefe

Department of Geosciences, King Fahd University of Petroleum & Minerals (KFUPM), P. O. Box 8082, Dharhan, Saudi Arabia. Phone: +966533584798, +2347038684403 Email: paul_edigbue@yahoo.com

Professional Overview

Objective: To secure a career in which the corporate culture and policies of the Company allow me to use my experience and knowledge in field of Geoscience.

Career Summary: Geophysicist who excels at analyzing, prioritizing and completing tasks in a professional manner.

Summary of Skills

- Good understanding of seismic data processing and Interpretation
- General knowledge of the oil and gas exploration and production industry
- Supportive and collaborative in a team environment
- Good computer literacy and readiness for multidisciplinary training
- Excellent technical and analytical skills
- Excellent communication and presentation skills

Education

| | |
|----------------------------------------------------------------------------------------------------------------------|------|
| Master of Science, Geophysics King Fahd University of Petroleum & Minerals – Dharhan, Saudi Arabia | 2015 |
| Master of Technology, Exploration Geophysics Federal University of Technology - Akure, Ondo, Nigeria | 2014 |
| Bachelor of Technology, Applied Geophysics Federal University of Technology - Akure, Ondo, Nigeria | 2008 |
| Higher National Diploma, Geophysics Technology Federal University of Technology/NIST- Akure, Ondo, Nigeria | 2004 |

Experience

| | |
|-----------------------------------------------------------------------------------------------------------|---------------------|
| Geophysicist Intern Seplat Petroleum Development Company Plc. Ikoyi, Lagos State. | 2014 |
| Geophysicist/Technologist (Oil & Gas) Federal University of Technology - Akure, Ondo State. | 2011 – 2013 |
| Geophysicist Abisdrill Nigeria Limited, Oke Ijebu, - Akure, Ondo State. | 2010 -- 2011 |

Professional Training and Short Course

- EAGE Distinguished Instructor Short Course (DISC) "Seismic Fracture Characterization: Concept and Practical Applications, Saudi Arabia, Feb. 2014.
- SEG Distinguished Instructor Short Course (DISC) "Making a Difference with 4D: Practical Applications of Time-Lapse Seismic Data, at Bahrain, 2013
- Petrel Introduction G & G Course, Organized by ExxonMobil, Lagos, Nigeria, 2012
- Imperial Barrel Award Training and Competition, AAPG Africa Region, 2012

Awards and Recognition

Second Best Oral Paper Presenter at 6th NAPE Mini-Conference, O. A. U., Ile-Ife, Osun State, Nigeria, April, 2012.

Certificate of Participation in “Imperial Barrel Award” African Region, March
Two Times Winner of The SEG foundation scholarship "Educational Award"

Sponsored by AGIP, 2006- 2008.

NYSC Certificate Of Commendation on Outstanding Performance, Feb. 2012

Certificate of Diligent Service, Government Day Junior Secondary School, Garin Alkali, Yobe State, Jan. 2010

Memberships/Scholarly Societies

Society Of Exploration Geophysicist (SEG), American Association of Petroleum Geologist (AAPG), Dharhan Geoscience Society (DGS), Nigeria Association of Petroleum Explorationist (NAPE), Nigeria Institute Of Science & Technology (NIST).

Additional Information

- Proficient in Geophysical Software such as PETREL™, Seismic Unix, OpendTect, Matlab, Mathematica, Winserve, Surfer, Resist, etc.

Publications

- Hydrocarbon reservoir characterization of "Keke" field, Niger Delta using 3D seismic and petrophysical data. (American Journal of Scientific And Industrial Research, 2014)
- Seismic stratigraphy and attribute analysis of an offshore field, Niger Delta, Nigeria (Arabian Journal of Geoscience, 2014)
- Integration of sequence stratigraphy and geostatistics in 3D reservoir modeling: a case study of Otumara Field, Onshore Niger Delta. (Arabian Journal of Geoscience, 2015)

Hobbies: Researching, Studying, Tackling new Challenges, Sports & Traveling.

Referees: *Available on Request*